The calcineurin regulator Sarah enables distinct forms of homeostatic plasticity at the *Drosophila* neuromuscular junction

Noah S. Armstrong[1,2] and C. Andrew Frank[1,2, 3]

[1]Department of Anatomy and Cell Biology, University of Iowa Carver College of Medicine, Iowa City, IA, United States; [2]Interdisciplinary Graduate Program in Neuroscience University of Iowa, Iowa City, IA, United States; [3]Iowa Neuroscience Institute, University of Iowa, Iowa City, IA

*** Correspondence:**

C. Andrew Frank

andy-frank@uiowa.edu

Keywords: *Drosophila melanogaster*, NMJ, neurotransmission, plasticity, synaptic homeostasis, synaptic dysfunction, calcineurin, *sarah* (*sra*)

Abstract

The ability of synapses to maintain physiological levels of evoked neurotransmission is essential for neuronal stability. A variety of perturbations can disrupt neurotransmission, but synapses often compensate for disruptions and work to stabilize activity levels, using forms of homeostatic synaptic plasticity. Presynaptic homeostatic potentiation (PHP) is one such mechanism. PHP is expressed at the *Drosophila melanogaster* larval neuromuscular junction (NMJ) synapse, as well as other NMJs. In PHP, presynaptic neurotransmitter release increases to offset the effects of impairing muscle transmitter receptors. Prior *Drosophila* work has studied PHP using different ways to perturb muscle receptor function – either acutely (using pharmacology) or chronically (using genetics). Some of our prior data suggested that cytoplasmic calcium signaling was important for expression of PHP after genetic impairment of glutamate receptors. Here we followed up on that observation. We used a combination of transgenic *Drosophila* RNA interference and overexpression lines, along with NMJ electrophysiology, synapse imaging, and pharmacology to test if regulators of the calcium/calmodulin-dependent protein phosphatase calcineurin are necessary for the normal expression of PHP. We found that either pre- or postsynaptic dysregulation of a *Drosophila* gene regulating calcineurin, *sarah* (*sra*), blocks PHP. Tissue-specific manipulations showed that either increases or decreases in *sra* expression are detrimental to PHP. Additionally, pharmacologically and genetically induced forms of expression of PHP are functionally separable depending entirely upon which *sra* genetic manipulation is used. Surprisingly, dual-tissue pre- and postsynaptic *sra* knockdown or overexpression can ameliorate PHP blocks revealed in single-tissue experiments. Pharmacological and genetic inhibition of calcineurin corroborated this latter finding. Our results suggest tight calcineurin regulation is needed across multiple tissue types to stabilize peripheral synaptic outputs.

INTRODUCTION

Normal synapse function permits a pre-determined physiological range of activity. Challenges to synapse function can force activity beyond setpoint limits. To maintain stability, synaptic and circuit level homeostatic mechanisms exist in vertebrates and invertebrates (Davis, 2006, Marder, 2012, Pozo and Goda, 2010, Frank, 2014a). Defects in homeostatic plasticity can impair the preservation of neuronal activity and may be associated with neurological conditions that display instabilities including ataxia, migraine, schizophrenia, Alzheimer's disease and epilepsy (Andre et al., 2018, Dickman and Wondolowski, 2013, Wondolowski and Dickman, 2013, Bliss et al., 2014). Synaptic homeostasis has also been implicated as being necessary for the manifestation of normal sleep behavior (Tononi and Cirelli, 2006, Kikuma et al., 2019). For these diverse behaviors or neurological disorders, the relevant synaptic activities and functional challenges operate on varying timescales, from minutes (e.g., perturbations that induce migraine) to years (e.g., conditions like Alzheimer's Disease). Yet there are significant gaps in understanding of how neuronal stability is maintained, across neural tissue types and over broad timescales.

We can address some of these gaps using model synapses, like the *Drosophila melanogaster* neuromuscular junction (NMJ). The *Drosophila* NMJ is a well-studied synapse (Menon et al., 2013). It is suitable for combining approaches in genetics, development, and electrophysiology (Jan and Jan, 1976). For homeostatic synaptic plasticity, the NMJ has been key for mechanistic discovery (Frank et al., 2020). One well-characterized form of homeostatic plasticity is called presynaptic homeostatic potentiation (PHP). In *Drosophila*, PHP is initiated when postsynaptic glutamate receptors are impaired, decreasing quantal size. The synapse detects this impairment, and a muscle-to-nerve signaling process drives increased presynaptic glutamate release. The prevailing model is that potentiated release happens after retrograde signaling triggers an increase in presynaptic calcium influx through Ca_V2 voltage-gated calcium channels (Frank et al., 2006, Frank et al., 2009, Müller and Davis, 2012, Wang et al., 2014, Younger et al., 2013). This increase in presynaptic calcium influx coincides with an increased readily releasable pool (RRP) of synaptic vesicles (Harris et al., 2015, Müller et al., 2015, Müller et al., 2012, Weyhersmüller et al., 2011). These modifications drive the ability of the motor neuron to deliver more glutamate to the cleft, offsetting the decreased quantal size.

67 PHP is studied using different kinds of manipulations. Acute inhibition of glutamate
68 receptors causes PHP to be expressed rapidly, in minutes (Frank et al., 2006). By contrast, genetic
69 manipulations last over extended developmental time (Davis et al., 1998, DiAntonio et al., 1999,
70 Petersen et al., 1997). Acute PHP can be induced and expressed by applying glutamate receptor
71 inhibitors, like Philanthotoxin-433 (PhTx) (Frank et al., 2006) or GYKI-53655 (Nair et al., 2021).
72 Alternatively, glutamate receptors can be impaired genetically using a loss of function mutation in
73 *GluRIIA*^{SP16} (Petersen et al., 1997), RNAi-mediated knockdown of *GluRIII* (Brusich et al., 2015), or
74 a variety of other manipulations that impair receptor expression throughout development
75 (reviewed in (Frank, 2014a)). Each of these manipulations results in decreased quantal size, offset
76 by increased quantal content, resulting in normal levels of evoked excitation.

77 In prior work, we reported that a signaling modality including Gq, Plc21C (*Drosophila*
78 PLCβ homolog), IP_3 receptors, and ryanodine receptors were necessary for the expression of PHP
79 after genetic glutamate receptor loss, but not after acute pharmacological PhTx challenge (James
80 et al., 2019). IP_3 receptors and ryanodine receptors have dual pre- and postsynaptic functions by
81 mediating the release of intracellular calcium from intracellular calcium stores (Kadamur and Ross,
82 2013, Philip et al., 2010). However, it is unknown which calcium-dependent molecules must be
83 activated or regulated via the release of calcium from intracellular stores to promote homeostatic
84 potentiation.

85 Calcineurin is a well conserved Ca^{2+}/calmodulin-dependent protein phosphatase that is
86 found in most mammalian tissues but is expressed at high levels in the brain, and it has been shown
87 to regulate ion channel function and trafficking, apoptosis, gene regulation, receptor trafficking,
88 neuronal plasticity, and immune processes (Rusnak and Mertz, 2000, Furman and Norris, 2014,
89 Musson and Smit, 2011, Baumgärtel and Mansuy, 2012). Calcineurin is also regulated by a family of
90 proteins known as regulators of calcineurin (RCAN1), which are the product of Down Syndrome
91 Critical Region 1 (DSCR1) gene (Park et al., 2009, Harris et al., 2005). There is evidence that suggests
92 that RCAN family members inhibit calcineurin activity (Kingsbury and Cunningham, 2000, Lee et al.,
93 2003). The *Drosophila* gene *sarah* (*sra*; also known as *nebula*) encodes the only known ortholog
94 of DSCR1 in *Drosophila* (Chang et al., 2003). Sra/Nebula/DSCR1 (herein: Sra) has been shown to
95 physically associate with the catalytic subunit of calcineurin (Takeo et al., 2006). Evidence suggests
96 that Sra inhibits calcineurin, as calcineurin activity has been shown to be approximately 40%

97 higher in *sra* mutants in comparison to controls or heterozygous mutants (Chang et al., 2003). *sra*
98 gene function has been shown to be required for mitochondrial function (Chang and Min, 2005),
99 female meiosis and egg activation (Takeo et al., 2006, Horner et al., 2006, Takeo et al., 2012), sleep
100 regulation (Nakai et al., 2011) and learning (Chang et al., 2003).

101 Here we report that either increases or decreases in *sra* gene expression – in either
102 presynaptic neuron or postsynaptic muscle – result in PHP impairment. Using genetics, we found
103 that different modes of PHP expression were functionally separable, as specific *sra* manipulations
104 compromised expression of PHP triggered by acute pharmacology or chronic genetic mutation.
105 We found that tissue-specific manipulations of *sra* resulted in strong blocks of PHP. But
106 surprisingly, dual tissue manipulations did not. Concurrent pre- and postsynaptic *sra* knockdown
107 or overexpression led to weaker (or no) blocks of PHP compared to single tissue impairments.
108 Consistent with this latter finding, global pharmacological inhibition of calcineurin via FK506
109 increases homeostatic capacity of the NMJ following a genetic PHP challenge.

110 Taken together, our data highlight a novel idea for homeostasis at the synapse. Regulatory
111 proteins like Sra are present in multiple synaptic tissues; if those factors are manipulated in tissue-
112 specific ways, there can be profound defects in overall synapse stability. But conversely, global
113 losses (or gains) of function may escape the most severe phenotypes. Our data set a framework for
114 testing how individual molecules contribute to homeostatic synaptic plasticity from different
115 synaptic tissues.

116

117 **METHODS**

118 ***Drosophila* husbandry and stocks**

119 *Drosophila melanogaster* fruit flies were raised on a standard cornmeal and molasses medium
120 prepared according to the recipe from the Bloomington *Drosophila* Stock Center (BDSC,
121 Bloomington, IN). *Drosophila* husbandry was performed according to standard practices
122 (Greenspan, 2004). Larvae were raised at 25ºC in humidity and light controlled (12 h light: 12 h
123 dark) Percival DR-36VL incubators (Geneva Scientific).

124 w^{1118} (Hazelrigg et al., 1984) was used as a non-transgenic wild type stock. The null
125 *GluRIIA*^{SP16} mutant generated previously (Petersen et al., 1997). The *UAS-GluRIII RNAi* line that
126 was used has been described previously (Brusich et al., 2015). GAL4 drivers that were used included
127 the neuronal drivers *elaV*(*C155*)-*GAL4* (Lin and Goodman, 1994) and *Sca-GAL4* (Budnik et al., 1996)
128 and the postsynaptic driver *BG57-GAL4* (Budnik et al., 1996). The *sra RNAi* line that was used was
129 *TRiP.JF02557* (BDSC:27260) (Shaw and Chang, 2013) and the *sra* overexpression line that was
130 used was *sra*^{EY07182} (BDSC:15991) (Lee et al., 2016). The *sra*^{Mi06435} was used alone (BDSC:42393)
131 and in conjunction with the deficiency line *Df(3R)sbd104* (BDSC:1920). The *CaNB RNAi* line that
132 was used was *TRiP.JF02616* (BDSC:27307) (Shaw and Chang, 2013).

133

134 **Electrophysiology and pharmacology**

135 Wandering third instar larvae were collected and dissected for NMJ analysis. Both control and
136 experimental conditions were performed in parallel using identical conditions. Dissections and
137 recordings were performed in a modified HL3 saline (70 mM NaCl, 5 mM KCl, 5mM HEPES, 10
138 mM $NaHCO_3$, 115 mM sucrose, 4.2 mM trehalose, 0.5 mM $CaCl_2$ (unless otherwise noted), 10
139 mM $MgCl_2$, pH 7.2 (Stewart et al., 1994). Neuromuscular junction sharp electrode recordings were
140 performed on muscles 6/7 of abdominal segments A2, A3, and A4. Miniature excitatory
141 postsynaptic potentials (mEPSPs) and excitatory postsynaptic potentials (EPSPs) were conducted
142 as previously described (Brusich et al., 2015, Spring et al., 2016, Yeates et al., 2017, James et al., 2019,
143 Mallik and Frank, 2022).

144 Uncorrected quantal content was calculated per NMJ by dividing the average EPSP by the
145 average mEPSP. Quantal content was then corrected for non-linear summation (NLS quantal
146 content) using the following calculation (McLachlan and Martin, 1981):

147 $$\bar{v'} = E \ln \frac{E}{(E - \bar{v})}$$

148 $\bar{v'}$ is the NLS corrected EPSP, E is the electromotive force (in this case equal to resting membrane
149 potential), and $\bar{v}$ is equal to the EPSP amplitude. To find NLS corrected quantal content, the
150 corrected EPSP amplitude ($\bar{v'}$) is then divided by mEPSP amplitude.

151 Recordings were performed on a Leica microscope using a 10x objective and acquired
152 using an Axoclamp 900A amplifier, Digidata 1440A acquisition system and pClamp10.7
153 (Molecular Devices) software. Data were analyzed using MiniAnalysis (Synaptosoft) and the
154 Clampfit (Molecular Devices) programs. To generate mEPSP and EPSP traces for figures, (x,y)
155 coordinates were pulled from the Clampfit program and imported into GraphPad Prism
156 (GraphPad) software. All traces display the recording that was at or closest to the calculated
157 average of each specific condition.

158 Pharmacological agents were bath applied in recording saline at the final concentrations
159 indicated in the text and figures. The agents included Philanthotoxin-433 (PhTx, Sigma-Aldrich),
160 Cyclosporin A (Sigma-Aldrich), and FK506 (InvivoGen).

161

162 **Immunostaining and analyses**

163 Wandering third instar larvae were dissected on a sylgard Petri plate in HL3 and fixed using
164 Bouin's fixative for 10 minutes or 4% paraformaldehyde in PBS for 30 minutes. Larvae were
165 washed with PBS containing 0.2% Triton X-100 (PBST) for 40 min, blocked for an hour with
166 2.5% BSA, and incubated overnight with primary antibodies at 4ºC. This was followed with
167 another 40 min of washes, and incubation in secondary antibodies for 1.5 hr at room temperature.
168 The primary antibodies used were mouse anti-Synapsin (anti-Syn; 3C11) 1:50 (Developmental
169 Studies Hybridoma Bank, Iowa City, IA); rabbit anti-Dlg 1:15,000 (Budnik et al., 1996); mouse
170 anti-phosphorylated CaMKII (pCaMKII) 1:100 (MA1-047; Invitrogen); rabbit anti-GluRIII 1:150
171 (Marrus et al., 2004, Goel and Dickman, 2018). The following fluorophore conjugated secondary
172 antibodies were also used (Jackson ImmunoResearch Laboratories): goat anti-mouse 488 1:1000
173 (DyLight) and goat anti–rabbit 549 1:2000 (DyLight). Larval preparations were mounted in
174 Vectashield (Vector Laboratories) and imaged at room temperature with a 700 Carl Zeiss laser
175 scanning confocal microscope equipped with 63 × /1.4 NA oil immersion objective using separate
176 channels with four laser lines (405, 488, 555, and 639 nm).

177 All quantifications were performed on muscle 6/7 segments A2 and A3. For NMJ growth
178 analysis, anti-Dlg boutons were counted in muscle after verifying that there was a corresponding
179 cluster of anti-Syn staining in motor neurons. For pCaMKII and GluRIII intensity measurements,

180 a mask was created around the GluRIII channel to define the postsynaptic region and eliminate
181 background. Only pCaMKII signals within this mask at Ib postsynaptic densities were quantified.
182 Images were prepared for publication using Adobe Illustrator.

183

184 **Statistical analyses**

185 Statistical significance was tested using either a Student's T-Test to compare one experimental
186 data set directly to a control data set or using a one-way ANOVA with a Tukey's post-hoc test if
187 multiple data sets were being compared. Specific *p*-value ranges used were as follows: *$p<0.05$,
188 **$p<0.01$, and ***$p<0.001$. All statistical analyses were conducted using GraphPad Prism
189 software. Data were plotted in GraphPad Prism and final figures were compiled using Adobe
190 Illustrator.

191

192 **RESULTS**

193 **Concurrent neuron and muscle *sra* knockdown do not block PHP**

194 PHP is commonly assessed at the *Drosophila* NMJ using acute Philanthotoxin-433 (PhTx)
195 application to test the rapid expression of PHP (Frank et al., 2006) or chronic genetic manipulations
196 to test the expression of PHP throughout life, like the $GluRIIA^{SP16}$ the genetic null mutation
197 (Petersen et al., 1997) or knock down of *GluRIII* gene function by RNAi (Brusich et al., 2015). All
198 of these manipulations result in decreased mEPSP amplitude while quantal content (corrected for
199 non-linear summation, herein NLS quantal content) increases. Evoked excitation is maintained as
200 a result. This indicates PHP mechanisms are working to sustain evoked potentials near normal
201 levels.

202 Given our prior data suggesting that dysregulation of calcium stores disrupted the
203 maintenance of PHP after genetic challenge (Brusich et al., 2015, James et al., 2019), we wanted to
204 test whether combined pre- and postsynaptic *sra* loss-of-function conditions impaired PHP. To do
205 this, we used a *Drosophila* line that contains both neuron and muscle GAL4 drivers to knockdown
206 *sra* using RNAi and applied 20µM PhTx to test rapid PHP expression. This *sra RNAi* line been

207 shown to knock down protein levels of Sarah (also known as Nebula) by about 60% (Shaw and
208 Chang, 2013).

209 PhTx application decreased mEPSP amplitude for both driver control and *sra RNAi*
210 conditions (**Figure 1A**) (Frank et al., 2006). Evoked potentials were maintained for the driver
211 control (**Figure 1B**) because of the compensatory significant increase in NLS quantal content
212 (**Figure 1C**). Dual tissue knockdown of *sra* resulted in a mild decrease in evoked potentials
213 following PhTx incubation. This might be consistent with a small defect in homeostatic plasticity,
214 but there was still a significant increase in NLS quantal content compared to non-drugged controls
215 (**Figure 1A-D** and **Supplementary Table 1**). At a minimum, this indicated partially intact acute
216 PHP expression.

217 To test for the maintenance of PHP, we first used a *Drosophila* line that contains both
218 neuron and muscle GAL4 drivers, along with *UAS-GluRIII RNAi* to provide a genetic homeostatic
219 challenge (Brusich et al., 2015). This *UAS-GluRIII RNAi* reagent is a good first-test or screening
220 tool to identify genes needed for the maintenance of PHP (Brusich et al., 2015). Again, while there
221 were significant decreases in evoked amplitude in *sra RNAi* synapses challenged with either PhTx
222 or *GluRIII RNAi*, there were still some compensatory increases in NLS quantal content (Figure
223 1A-D). Our interpretation of these data is that PHP mechanisms are partially (or largely) intact
224 when *sra* function is knocked down.

225

226 **Concurrent neuron and muscle *sra* overexpression do not block PHP**

227 We acquired reagents to test if simultaneous pre- and postsynaptic overexpression of *sra* resulted
228 in impairment in forms of PHP. We used the $sra^{EY07182}$ allele. This is a 5' P-element insertion allele
229 in the endogenous *sra* locus with *UAS* binding sites for GAL4 transcriptional control upstream of
230 the *sra* gene; this allows for conditional tissue specific overexpression of *sra*. Overexpression of
231 *sra* neuronally using the pan neuronal driver, *elaV*, and $sra^{EY07182}$ has been shown to result in
232 transcript levels that were approximately twofold higher than controls (Lee et al., 2016).

233 For our electrophysiological experiments, there was a decrease in the EPSPs of neuron +
234 muscle GAL4 >> $sra^{EY07182}$ ("*sra* OE" - overexpression) + *GluRIII RNAi* synapses compared to
235 neuron + muscle GAL4 >> $sra^{EY07182}$ alone, and there was only a small – but not statistically

236 significant – increase in NLS quantal content (**Figure 1E-H** and **Supplementary Table 1**). Our
237 interpretation of these data is that the chronic expression of PHP is not fully intact. Additionally,
238 we there was no significant difference in the EPSPs of neuron + muscle GAL4 >> *sra*^{EY07182}
239 overexpression animals alone or genetically identical overexpression animals challenged with
240 PhTx (**Figure 1E-H**). Taken as a whole, concurrent overexpression of *sra* both pre-and
241 postsynaptically does not appear to block homeostatic responses at the NMJ. If anything,
242 phenotypes are subtle, indicating partial impairments of PHP.

243

244 **Global *sra* mutation shows a mixed PHP phenotype and deficient neurotransmission at low**
245 **calcium**

246 We turned to mutant *Drosophila* stocks to examine loss-of-function alleles. We used the *sra*^{Mi06435}
247 transposon insertion to test if a global disruption of *sra* function would block PHP or show
248 defective neurotransmission. We compared *sra*^{Mi06435} alone to wild type and *sra*^{Mi06435} over
249 chromosomal deficiency (*Df*). We found no significant differences in EPSP amplitude or NLS
250 quantal content between any groups (**Figure 2A-C** and **Supplementary Table 2)**, indicating a
251 normal level of baseline neurotransmission.

252 To challenge the mutant NMJs and test for PHP, we used a *GluRIIA*^{SP16} null mutant
253 (Petersen et al., 1997) and combined it with the *sra*^{Mi06435}*/Df* allelic combination. The addition of
254 the *GluRIIA*^{SP16} mutation caused a significant decrease in mEPSP amplitude, as expected (**Figure**
255 **2A**). Yet our test for PHP expression was mixed. This is because in the *sra* loss-of-function
256 combination, the homeostatic challenge was coupled with a small, but not statistically significant
257 decrease in EPSP amplitude (**Figure 2B**) and a small, but not significant increase in NLS quantal
258 content (**Figure 2C**). If there were robust PHP for the *sra* mutants, one would predict an increase
259 in quantal content in response to the homeostatic pressure of decreased mEPSPs. Conversely, if
260 there were blocked PHP, one would expect a decrease in EPSP amplitude. Neither occurred.

261 Prior studies showed that mutants with intermediate PHP phenotypes can be sensitive to
262 levels of calcium (Frank, 2014a, Frank, 2014b, Genç and Davis, 2019, Frank et al., 2006). Therefore, we
263 also examined *sra*^{Mi06435} and *sra*^{Mi06435}*/Df* for defective neurotransmission in low calcium
264 conditions (0.20mM). Somewhat surprisingly, *sra*^{Mi06435} and *sra*^{Mi06435}*/Df* showed decreased

265 mEPSP amplitude and EPSP amplitude compared to wild type, and no increase in NLS quantal
266 content (**Figure 2E-G**). Our *sra*^{Mi06435} and *sra*^{Mi06435}/*Df* data lead us to the interpretation that PHP
267 and NMJ function are highly sensitive to low levels of calcium. This is a phenotype shared with
268 some other homeostatic factors that govern presynaptic release (Frank, 2014b, Frank et al., 2006,
269 Yeates and Frank, 2021).

270

271 **Postsynaptic *sra* knockdown impairs the rapid expression of PHP but not its maintenance**

272 After testing for dual-tissue functions for *sra* in PHP, we conducted single-tissue experiments.
273 First, we used the *UAS-sra RNAi* transgene to knockdown *sra* expression in the muscle. We applied
274 PhTx to animals that expressed *UAS-sra RNAi* in the muscle using the GAL4 driver, *BG57-GAL4*.
275 Surprisingly, in contrast to the dual-tissue knockdown, postsynaptic knockdown of *sra* completely
276 blocked the rapid expression of PHP, resulting in significantly decreased EPSP amplitudes and a
277 failure to show a compensatory increase in NLS quantal content (**Figure 3B,C** and
278 **Supplementary Table 3**). We tested the if the postsynaptic knockdown of *sra* would also block
279 of the chronic maintenance and expression of PHP. Knockdown of *sra* postsynaptically in a
280 *GluRIIA*^{SP16} background not only exhibited an expected decrease in mEPSP amplitude compared
281 to non-*GluRIIA*^{SP16} controls, but also a marked decrease in EPSP amplitude (**Figure 3E,F** and
282 **Supplementary Table 3**). There was a slight but significant increase in quantal content, which
283 indicates partially intact PHP mechanisms (**Figure 3G**).

284 Our results are consistent with the idea that the knockdown of *sra* postsynaptically induces
285 a complete block when acutely challenged with pharmacology, but only a partial block when
286 chronically challenged genetically. This suggests that the postsynaptic expression of *sra* may have
287 a differential role in regulating two separable forms of PHP. We tested this idea further.

288

289 **Postsynaptic *sra* overexpression blocks the maintenance of PHP but not acute expression**

290 After examining postsynaptic *sra* knockdown, we did the opposite genetic perturbation: we
291 examined overexpression of *sra* postsynaptically. We found that applying PhTx to synapses with
292 *sra* overexpressed postsynaptically reveals partially impaired rapid PHP expression (**Figure 4A-**

293 **D** and **Supplementary Table 4**). There was no significant difference in EPSPs between
294 unchallenged and challenged NMJs. There was a small numerical increase in NLS quantal content,
295 but this increase did not achieve statistical significance (**Figure 4C**).

296 Next, we tested if postsynaptic overexpression of *sra* could block chronic expression of
297 PHP using the $sra^{EY07182}$ allele in a $GluRIIA^{SP16}$ background. Overexpression of *sra*
298 postsynaptically yielded normal baseline EPSP amplitude (as in Figure 1), but this postsynaptic
299 overexpression of *sra* in $GluRIIA^{SP16}$ null NMJ background triggered a significant decrease in
300 EPSP amplitude along with a failure to increase NLS quantal content when compared to the
301 unchallenged control (**Figure 4E-H** and **Supplementary Table 4**). In fact, the NLS quantal
302 content was also significantly decreased in the $GluRIIA^{SP16}$ background, which is not a common
303 phenotype. This is indicative a strong block of chronically expressed PHP. Taken together, our
304 data suggest that proper postsynaptic expression of *sra* is critical for the NMJ to respond to
305 different kinds of PHP challenge.

306

307 **Postsynaptic *sra* overexpression does not impair synapse development**

308 Since the postsynaptic overexpression phenotype was the strongest, we checked if it
309 correlated with NMJ developmental defects. In principle, synaptic developmental defects could
310 explain the physiological phenotypes. We immunostained third instar larval *Drosophila* NMJs for
311 presynaptic boutons to quantify their elaboration. We overexpressed *sra* postsynaptically alone
312 and or in conjunction with $GluRIIA^{SP16}$. We visualized NMJ bouton development in synapse 6/7
313 muscle segments A2 and A3 by co-staining with anti-Synapsin (Syn, presynaptic vesicle marker)
314 and anti-Discs Large (DLG, postsynaptic density marker).

315 We did not find marked differences in bouton number between any group for NMJ 6/7
316 within segment A2 or segment A3 (**Figure 5A-G** and **Supplementary Table 5**) (segments
317 analyzed separately due to documented differences in development). We quantified bouton
318 normalized per muscle area and found that postsynaptic overexpression of *sra* resulted in a
319 significant increase compared to other genotypes (**Figure 5H** and **Supplementary Table 5**). This
320 indicates that *sra* overexpression in the muscle may result in smaller muscles – but in any case,
321 these unchallenged animals had intact physiology (**Figure 4**). These data indicate that postsynaptic

322 overexpression of *sra* does not impair gross NMJ development, and therefore, a developmental
323 defect unlikely to be contributing towards the observed PHP block by electrophysiology. The
324 caveat to this experiment is that more subtle developmental changes are possible on the level of
325 active zones or glutamate receptor clusters. We decided to examine a marker known to correlate
326 with PHP expression at a specific motor terminal.

327

328 **Overexpression of *sra* postsynaptically disrupts pCaMKII downregulation in Ib motor**
329 **neurons**

330 To try to gain more mechanistic understanding of how postsynaptic *sra* overexpression may be
331 blocking the maintenance of PHP, we measured phosphorylated CaMKII (pCaMKII) levels and
332 glutamate receptor signal intensity. Genetic glutamate receptor challenges normally result in
333 decreased levels of pCaMKII immunofluorescence (Kikuma et al., 2019, Goel et al., 2017, Li et al.,
334 2018, Newman et al., 2017), and this decrease correlates with successful expression of PHP.

335 We measured pCaMKII intensity at Ib postsynaptic densities. We found a significant
336 decrease in *GluRIIA*^{SP16} animals compared to wild-type animals as has been shown previously
337 (**Figure 6A,B** and **Supplementary Table 6**). We note for this experiment that our muscle driver
338 control lines also showed unexpected decreases in baseline pCaMKII and GluRIII staining
339 compared to wild type (**Figure 6A,B**). These effects are likely due to the genetic background of
340 the driver, but they are important for subsequent comparison with *sra* overexpression.

341 Surprisingly, when comparing overexpression of *sra* postsynaptically to overexpression of
342 *sra* postsynaptically in *GluRIIA*^{SP16} null NMJs, we not only failed to see a decrease in pCaMKII
343 intensity, but we saw a significant increase (**Figure 6A,B**). Moreover, when examining GluRIII
344 (also known as GluRIIC) intensity, we saw no significant difference between wild type and
345 *GluRIIA*^{SP16} (**Figure 6A,C**). However, we saw a significant increase in GluRIII intensity in *sra*
346 postsynaptic overexpression in the *GluRIIA*^{SP16} null background when compared to *sra*
347 overexpression alone or wild type (**Figure 6A,C**). It is possible that the synapse (unsuccessfully)
348 attempted to compensate for its electrophysiological deficits by trafficking in more glutamate
349 receptors.

350

351 **Knockdown of *sra* presynaptically impedes the maintenance of PHP but not acute expression**

352 Because we saw strong tissue-specific phenotypes when genetically dysregulating *sra* in the
353 muscle, we tested if knockdown of *sra* presynaptically also affected PHP. Acute application of
354 PhTx to NMJs with *sra* neuronal knockdown did not block Acute PHP expression as EPSP
355 amplitudes were mostly maintained, and NLS quantal content was significantly increased between
356 challenged and unchallenged animals (**Figure 7A-D** and **Supplementary Table 7**).

357 To understand if decreasing *sra* expression presynaptically blocks the long-term expression
358 of PHP, we turned to the $GluRIIA^{SP16}$ null mutant again. We found that decreased *sra* expression
359 neuronally blocked chronic PHP because of decreased EPSP amplitude in $GluRIIA^{SP16}$, *sra RNAi*
360 NMJs when compared to $GluRIIA^{SP16}$ or *sra RNAi* alone (**Figure 7E-H** and **Supplementary Table**
361 **7**). The $GluRIIA^{SP16}$, *sra RNAi* synapses also failed to show a significant increase in NLS quantal
362 content compared to the unchallenged control (**Figure 7G**). This provides us with evidence that
363 the knockdown of *sra* presynaptically blocks the long-term maintenance phase of PHP

364

365 **Overexpression of *sra* presynaptically blocks long-term PHP expression**

366 Finally, we tested if the presynaptic overexpression of *sra* affects PHP. After applying PhTx to
367 NMJs with *sra* neuronal overexpression, we did not find any significant differences in evoked
368 amplitude while getting a robust increase in NLS quantal content (**Figure 8A-D** and
369 **Supplementary Table 8**).

370 Next, we attempted to test chronic PHP expression following neuronal *sra* overexpression
371 in a $GluRIIA^{SP16}$ null background. There was a statistically significant decrease in the evoked
372 amplitudes of *elaV(C155)-Gal4 >>* $sra^{EY07182}$ synapses and a non-significant NLS quantal content
373 increase (**Figure 8E-H** and **Supplementary Table 8**). Yet based on our controls, we cannot
374 attribute those data to *sra* overexpression alone: this is because the neuronal driver in this
375 experiment also seemed to contribute to the phenotype **(Figure 8F-H)**.

376

377 **FK506 reverses the effects of postsynaptic overexpression of *sra***

378 We were puzzled why the single-tissue genetic manipulations of *sra* yielded stronger PHP
379 inhibition. One possibility is that for instances where a molecule normally functions in multiple
380 tissues, synapses could engage homeostatic systems to cope with a global loss (e.g., endogenous
381 genetic mutation) of that molecule. In principle, challenging a synapse with single tissue genetic
382 manipulation could disrupt this process.

383 Our earlier experiments showed a strong chronic PHP block when *sra* was overexpressed
384 postsynaptically (**Figure 4E-H** and **Supplementary Table 4**). Sra is a calcineurin inhibitor. Thus,
385 overexpressing the *sra* gene (*sra* OE) postsynaptically should decrease calcineurin activity in
386 muscle. If the above model is correct, then impairing calcineurin globally via a pharmacological
387 calcineurin inhibitor could reverse the chronic PHP block.

388 FK506 (tacrolimus) is a calcineurin inhibiting drug that binds to FK-binding protein l (Liu
389 et al., 1991, Sigal and Dumont, 1992, Clardy, 1995). This immunophilin-drug binds to calcineurin and
390 inhibits its protein phosphatase activity (Kuromi et al., 1997, Clardy, 1995, Swanson et al., 1992). There
391 are notable phenotypes at synaptic preparations. For whole-cell patch clamp in rat cortex,
392 application of FK506 increased the frequency of spontaneous events (Victor et al., 1995). And
393 application of FK506 to *Drosophila* larval neuromuscular junctions has been reported to increase
394 the endocytosis of synaptic vesicles, while having no effect on the frequency of spontaneous events
395 or the mean amplitude of evoked events (Kuromi et al., 1997), though the specificity of FK506 in
396 impairing calcineurin at the *Drosophila* NMJ has not been thoroughly documented.

397 We repeated the experiment of overexpressing *sra* in the muscle, this time incubating NMJ
398 preps with FK506. Larval preps were incubated with 50μM FK506 for 15 minutes prior to
399 electrophysiological recordings. We replicated our earlier finding that *sra* muscle overexpression
400 challenged with the $GluRIIA^{SP16}$ null mutation showed decreased evoked amplitude and a marked
401 decrease NLS quantal content, instead of an increase (**Figure 9B,C** and **Supplementary Table 9**).
402 We also repeated our driver controls, and we should note that in the case of this set of experiments,
403 the driver also appeared to confer an impairment of PHP (**Figure 9B,C and Supplementary Table**
404 **9**) – though consistent with before (**Figure 4**), the effect was not nearly as severe as with *sra*
405 muscle overexpression.

406 Genetically identical animals were incubated with FK506. We found that EPSP amplitude
407 is significantly and specifically increased in the *sra* muscle overexpression challenged with the

408 *GluRIIA*^{SP16} null mutation – compared to non-drugged controls – and this is a result of increased
409 NLS quantal content (**Figure 9A-D** and **Supplementary Table 9**). This experiment suggests that
410 global inhibition of calcineurin across tissues can mitigate the chronic PHP block caused by single
411 tissue *sra* manipulation. Alternatively, our results may point toward non-specific potentiation
412 presynaptically, induced by FK506. This latter possibility did not seem likely due to the specificity
413 of the effect on the *sra* overexpression line, but we conducted further tests.

414

415 **FK506 reverses the effects of presynaptic knockdown of *sra***

416 We wondered if we could reverse other PHP defects by pharmacologically blocking calcineurin.
417 We saw a block in chronic PHP following *sra* knockdown presynaptically (**Figure 7E-H**). We
418 repeated this experiment while also including synapses incubated with FK506. As before, in the
419 drug-free condition, EPSP amplitudes were deficient following *sra* presynaptic knockdown
420 challenged via *GluRIIA*^{SP16} and failed to increase NLS quantal content (**Figure 10B,C**). However,
421 incubation with FK506 significantly increased EPSP amplitude in these animals, and this was
422 accompanied by a robust increase in NLS quantal content (**Figure 10A-D** and **Supplementary**
423 **Table 10**). This provides further support that inhibition of calcineurin in a non-tissue-specific
424 pharmacological manner can reverse defects resulting from single tissue *sra* impairments and
425 restore PHP.

426

427 **Pharmacological inhibition of calcineurin generally improves homeostatic capabilities in**
428 **response to chronic PHP challenge**

429 We next tested if the pharmacological inhibition of calcineurin alone would also block PHP. We
430 applied FK506 to *GluRIIA*^{SP16} animals at either 10μM or 50μM concentrations. We saw no change
431 in EPSP amplitude in wild-type animals with drug application at either concentration, but
432 interestingly, in *GluRIIA*^{SP16} animals, we saw an increase in EPSP amplitude and NLS quantal
433 content following 50μM FK506 incubation compared to non-drugged controls (**Figure 11B** and
434 **Supplementary Table 11**). The 50μM concentration also produced increases in mEPSP frequency
435 in both wild type and *GluRIIA*^{SP16} animals (**Figure 11D** and **Supplementary Table 11**). These

436 data are consistent with our hypothesis that global inhibition of calcineurin may create scenarios
437 at the NMJ that are favorable to the expression of PHP.

438 We tested if FK506 increases release probability on its own. To do this, we conducted a
439 failure analysis in very low calcium (0.14mM) (Frank et al., 2006, Petersen et al., 1997). In extremely
440 low calcium, many presynaptic events fail to release vesicles and therefore fail to generate an
441 EPSP. In these low calcium conditions, probability of vesicle release is low (Del Castillo and Katz,
442 1954). Our failure analysis on wild-type and *GluRIIA*^{SP16} animals with and without FK506
443 incubation showed that FK506 significantly decreases the number of failures compared to non-
444 drugged controls (**Figure 11E** and **Supplementary Table 11**). Additionally, successful evoked
445 events were significantly bigger in amplitude (on average) after FK506 incubation compared to
446 non-drugged controls (**Figure 11F**). Taken together, these data suggest that FK506 increases
447 release probability. This may be occurring because of calcineurin inhibition increasing presynaptic
448 calcium either via influx from voltage-gated channels or efflux via intracellular stores.

449 As shown in our failure analysis experiment, FK506 can increase the EPSP amplitude in
450 wild-type animals in low calcium (**Figure 11F** and **Supplementary Table 11**). While there were
451 no changes at our standard calcium concentration of 0.5mM (**Figure 11B**), it is possible that at our
452 standard calcium concentration, we are having a "ceiling effect" where the application of FK506
453 may not be able to increase the EPSPs any further due to electromotive driving forces. To test this
454 idea, we conducted an experiment in 0.20mM Ca^{2+} in both wild type and *GluRIIA*^{SP16} animals with
455 and without FK506. As we predicted, the lower calcium concentration allowed us to detect an
456 increase in evoked amplitude and NLS quantal content in both genotypes following incubation
457 with FK506 (**Figure 11H,I** and **Supplementary Table 11**). This supports the idea that
458 pharmacological calcineurin inhibition may be potentiating calcium levels to increase release
459 probability.

460

461 **Postsynaptic knockdown of the calcineurin encoding gene *CaNB* blocks PHP maintenance**

462 Finally, we tested if genetic knockdown of a calcineurin subunit led to similar blocks in PHP as
463 observed with our *sra* manipulations. In *Drosophila*, there are three genes that encode the catalytic
464 subunit, CN A (*CaNA1*, *Pp2B-14D*, and *CaNA-14F*) and two genes that encode the regulatory

465 subunit, CN B (*CaNB* and *CaNB2*) (Takeo et al., 2006). *CaNA14-F* and *Pp2B-14D* share 82%
466 protein sequence identity and share approximately 62% identity with *CaNA1*, while *CaNB* and
467 *CaNB2* share 98% similarity in protein sequence (Tomita et al., 2011). Presynaptic knockdown of
468 *CaNB* leads to increased frequency of ectopic neuromuscular contacts, and *CaNB* knockouts have
469 been shown to have significantly reduced sleep (Nakai et al., 2011, Vonhoff and Keshishian, 2017).
470 Knockdown of *CaNB* reduces calcineurin activity, similar to *sra* overexpression (Lee et al., 2016,
471 Shaw and Chang, 2013).

472 We tested whether combined pre- and postsynaptic *CaNB* conditions impaired PHP, like
473 how we tested *sra* overexpression conditions (**Figure 1**). Dual tissue knockdown of *CaNB* resulted
474 in a mild decrease in evoked potentials following PhTx incubation, and there was a slight but
475 insignificant increase in NLS quantal content (**Figure 12A-D** and **Supplementary Table 12**).
476 When testing the maintenance of PHP using *UAS-GluRIII RNAi*, dual tissue knockdown of *CaNB*
477 did not impair evoked potentials and showed a robust increase in NLS quantal content. Taken
478 together, these data suggest a weak effect of *CaNB* dual tissue knockdown on acute PHP
479 expression and no effect on long-term PHP maintenance.

480

481 **DISCUSSION**

482 In this study, we provide a framework for understanding how a protein residing in different
483 synaptic tissues can contribute to Presynaptic Homeostatic Potentiation (PHP). The core finding
484 is that a single gene encoding a calcineurin regulator can regulate PHP in multiple ways, in
485 different tissues, and over various periods of time throughout the life of the synapse. Our work
486 offers a way to consider how overall synaptic stability is maintained through different kinds of
487 challenges to synapse function.

488 We show that concurrent neuronal and muscle knockdown or overexpression of *sra,* a
489 gene encoding a calcineurin regulator, does not strongly impair synaptic homeostatic
490 compensation mechanisms (**Figure 1**). Global genetic mutation of *sra* does not impair homeostasis
491 either, but it does reveal that the mutant synapse is sensitive to low levels of extracellular calcium
492 (**Figure 2**). Impairing *sra* in tissue-specific manners leads to numerous blocks in PHP.

493 In the muscle, postsynaptic knockdown of *sra* disrupts acute, PhTx-induced PHP (**Figure**
494 **3**) while postsynaptic overexpression strongly blocks expression PHP induced by *GluRIIA* loss
495 (**Figure 4**). We checked if developmental defects might be associated with that strong PHP
496 impairment. Postsynaptic overexpression of *sra* does not alter gross NMJ development (**Figure**
497 **5**), but it does cause an increased amount of pCaMKII apposing type-Ib boutons in a *GluRIIA*
498 mutant background (**Figure 6**).

499 For the neuron, we saw that presynaptic knockdown of *sra* blocks chronic PHP **(Figure 7**)
500 and presynaptic overexpression also impairs it (**Figure 8**). Additionally, we were able to alleviate
501 observed PHP blocks via FK506, which is a calcineurin inhibitor (**Figures 9, 10**). We also showed
502 that the maintenance of PHP can be further potentiated via FK506, especially when the system is
503 crippled by low extracellular calcium (**Figure 11**). Finally, we demonstrated that concurrent
504 neuronal and muscle knockdown of the calcineurin subunit *CaNB* led to a weak block in acute
505 PHP (**Figure 12**).

506

507 **Pre- vs. Postsynatpic Balance of a Homeostatic Factor**

508 The full complement of pre- and postsynaptic data is complex. One model is that the relative
509 balance of calcineurin function at NMJ tissues may control homeostatic signaling capacity. It is
510 possible that impairing *sra* either pre- or postsynaptically (separately) leads to a PHP block as it
511 can disrupt the relative amounts of calcineurin activity between the two sides of the synapse. This
512 idea could explain why a combined pre- and postsynaptic *sra* impairment (or a global
513 pharmacological impairment of calcineurin) may not block PHP. Even though calcineurin activity
514 is changed, the changes are reciprocal between both neuron and muscle.

515 To our knowledge, this type of idea (relative pre- or postsynaptic balance) is new to the
516 field of homeostatic plasticity. But it is reminiscent of prior ideas that have emerged from studies
517 of Hebbian plasticity. One example is the Bienenstock-Cooper-Munro (BCM) rule for visual
518 cortex learning. The BCM rule dictates that either potentiation or depression can occur, but the
519 direction of plasticity ultimately depends upon the level of postsynaptic activity after a presynaptic
520 neuron fires (Bienenstock et al., 1982). By contrast, if activity is globally impaired (e.g., by blocking
521 glutamate receptors), no directional plasticity is possible (Bienenstock et al., 1982). In our case, we

522 have an opposite kind of phenomenon. Block of glutamate receptors initiates a form of homeostatic
523 plasticity. The expression of that plasticity can be blocked by tissue-specific manipulations to
524 calcineurin – but not global manipulations.

525

526 **Potential neuronal mechanisms for *sra* regulation of calcineurin to impact PHP**

527 Calcineurin regulation is the most notable function of *sra*. Decreased expression of *sra* increases
528 calcineurin activity, while increased *sra* via overexpression is presumed to decrease it (Chang et
529 al., 2003, Shaw and Chang, 2013). Both of these types of manipulations are relevant in neuronal
530 expression of PHP (**Figures 7, 8**).

531 Calcineurin has several presynaptic roles in various models that have been shown including
532 affecting synaptic vesicle exocytosis and endocytosis, axon remodeling and regulating
533 neurotransmitter release (Tarasova et al., 2018). One target of presynaptic calcineurin is to
534 dephosphorylate Synapsin 1 which can affect the mobilization of synaptic vesicles from the reserve
535 pool to active zones (Cesca et al., 2010, Jovanovic et al., 2001, Chi et al., 2003). For those studies,
536 opposing interactions between calcineurin and various kinases regulate vesicle mobilization. This
537 may explain why neuronal *sra* overexpression impaired acute PHP because increased *sra*
538 decreases calcineurin activity which may impair the mobilization of vesicles to active zones.
539 Challenges to NMJ function (e.g., $GluRIIA^{SP16}$ or PhTx) consistently increase the number of
540 vesicles that are released, and failure to mobilize enough vesicles in response to a challenge may
541 lead to a failure for compensatory NLS quantal content increase and impair evoked release.

542 There are conflicting results on how the use of calcineurin inhibitors affects exocytosis.
543 They have been shown to increase the rate of exocytosis, show no change at all, or suppress
544 exocytosis (Yakel, 1997, Sim et al., 2003, Kumashiro et al., 2005). Specifically in the *Drosophila* NMJ,
545 calcineurin inhibition via FK506 has been shown to increase the endocytosis of synaptic vesicles,
546 while having no effect on the frequency of spontaneous events or the mean amplitude of evoked
547 events (Kuromi et al., 1997). This is contrary to the results of the current study where we showed
548 that mEPSP frequency is increased following FK506 incubation (**Figure 11D**). This difference
549 may be explained by the differences in concentration of FK506 that was used as previously, only
550 5μM and 10μM were tested. We see no change in mEPSP frequency at 10μM FK506, like previous

551 work as we only see the increase in spontaneous event frequency following 50μM FK506.
552 Alternatively, it is formally possible that FK506 could have some off-target effects at the NMJ that
553 affect parameters like mini frequency. Some possible ER-localized off-targets that could do this
554 are the ryanodine receptors (Ahern et al., 1994, Bultynck et al., 2000).

555 Calcineurin is believed to be a calcium-dependent regulator of endocytosis at both neuronal
556 and non-neuronal secretory cells (Wu et al., 2014). Calcineurin inhibitors slow endocytosis in
557 response to a small calcium influx but does not alter the speed of endocytosis in response to a large
558 calcium influx. If calcineurin is inhibiting synaptic vesicle recycling, this may explain why we see
559 a defect in chronic PHP following neuronal *sra* knockdown. Knockdown of *sra* leads to increased
560 calcineurin activity, and therefore increase inhibition of vesicular recycling. While this may not
561 lead to abnormal neurotransmission in the absence of a challenge, evoked amplitude may not be
562 maintained when chronically challenged due to an increased need for vesicle recycling in response
563 to the challenge.

564 Calcineurin may be affecting calcium influx as the targets of calcineurin in mouse NMJ
565 are L-type calcium channels (Gaydukov et al., 2013). Specifically, it was shown that calcineurin
566 downregulates neurotransmitter release by suppressing L-type calcium channels and calcium
567 release from intracellular stores through ryanodine receptors. In the *Drosophila* NMJ, it has
568 recently been shown that while L-type calcium channels are localized around active zones and
569 contribute to AP-triggered calcium influx, they are dispensable for evoked release (Krick et al.,
570 2021). However, it has not been shown if these channels are necessary for homeostatic signaling
571 processes. Calcium influx increases in response to both acute and chronic challenges to the synapse
572 (Müller and Davis, 2012). L-type calcium channels may be necessary for homeostatic compensation
573 as they not only serve as an additional entry point of calcium into the presynaptic compartment to
574 contribute to neurotransmitter release, but calcium entry through these channels also induces
575 calcium release from intracellular stores. In the current study, presynaptic loss of *sra* could lead to
576 increased calcineurin which may lead to increased inhibition of L-type calcium channels and not
577 allow for a large enough compensatory increase in calcium influx necessary to respond to a
578 homeostatic challenge.

579

580 **Possible postsynaptic mechanisms of *sra* to affect PHP through calcineurin regulation**

581 We also showed muscle roles for Sarah at the NMJ. Postsynaptic *sra* knockdown impaired acute
582 homeostatic signaling (**Figure 3**) while postsynaptic *sra* overexpression strongly blocked chronic
583 homeostatic signaling (**Figure 4**).

584 It is known that postsynaptic calcineurin activation can lead to the dephosphorylation of
585 AMPA receptors that can lead to the internalization of them (D'Amelio et al., 2011, He et al., 2009,
586 Lin et al., 2000). Ionotropic glutamate receptor subunits that are localized to muscle in *Drosophila*
587 are *DGluRIIA* and *DGluRIIB*, both of which are AMPA/kainite type receptors (Betz et al., 1993,
588 Petersen et al., 1997). This presents a potential mechanism for how *sra* knockdown in the muscle
589 blocks PHP- decreased *sra* expression increases calcineurin activity which may lead to increased
590 internalization of postsynaptic glutamate receptors. A decrease in the amount of available
591 glutamate receptors may be detrimental when glutamate receptors are already being challenged
592 via philanthotoxin. However, we showed that the amount of GluRIII is increased in animals with
593 postsynaptic overexpression of *sra* (**Figure 6**). Our data suggest that *sra* overexpression
594 postsynaptically triggers a system to compensate for increased pCaMKII levels by trafficking in
595 more glutamate receptors to Ib boutons.

596 Our study also showed an increase in pCaMKII at Ib postsynaptic densities following
597 overexpression of *sra* postsynaptically in the chronically challenged $GluRIIA^{SP16}$ null background
598 (**Figure 6**). Calcineurin is known to dephosphorylate I-1 which activates PPI to in turn
599 dephosphorylate and inactivate CaMKII (Tarasova et al., 2018). In the *Drosophila* NMJ, pCaMKII
600 levels have been found to be decreased following genetic glutamate receptor impairment (Newman
601 et al., 2017, Li et al., 2018, Goel et al., 2017). Additionally, postsynaptic overexpression of the
602 constitutively active phosphor-mimetic form of $CaMKII^{T287D}$ blocks chronic PHP expression (Li et
603 al., 2018). Chronic overexpression of *sra* in the muscle decreases calcineurin function, which may
604 be leading to an increased amount of pCaMKII, contrary to what normally occurs in response to a
605 homeostatic challenge. Our data provides correlative evidence that pCaMKII levels signal PHP
606 expression state, but mechanistically, it is unclear how decreased pCaMKII contributes to PHP. It
607 has been shown that mutations that alter CaMKII can impair the elaboration of the postsynaptic
608 subsynaptic reticulum and in turn result in defective PHP (SSR) (Koles et al., 2015, Koh et al., 1999).

609 It will be interesting to test how Sarah may interact with the development of the SSR and more
610 broadly how decreases in pCaMKII contribute to PHP.

611 It is likely that Sarah's impact on PHP is at least partly through its role in calcineurin
612 regulation. Dual-tissue knockdown of the calcineurin subunit *CaNB* partly impairs the acute phase
613 of PHP (**Figure 12**). Calcineurin and CaMKII have been shown to act as a switch-like mechanism
614 both for controlling the direction of calcium dependent growth cone tuning and for the regulation
615 of cofilin activity and subsequently actin cytoskeletal reorganization (Wen et al., 2004, Zhao et al.,
616 2012). It is possible that at the *Drosophila* NMJ, calcineurin and CaMKII act as a switch for
617 regulating postsynaptic signaling that is necessary for PHP maintenance.

618

619 **How *sra* could affect PHP through non-calcineurin regulating roles**

620 Previous work in rat cortex suggests that RCAN1 expression is upregulated following incubation
621 with Aβ (Lloret et al., 2011). The authors proposed that RCAN1 proteins not only inhibits
622 calcineurin but can also shift tau to a hyperphosphorylated state via inducing expression of GSK3β.
623 This provides evidence that RCAN1 proteins are linked to Alzheimer's and neurodegeneration.
624 Like this work and human studies, Aβ42-expressing *Drosophila* show increased Sra levels in the
625 brain (Lee et al., 2016). Genetic overexpression of *sra* in combination with Aβ42 impaired
626 locomotor activity and lifespan compared to overexpression of *sra* alone. However, data from
627 *Drosophila* suggest that upregulation of *sra* can be neuroprotective in the presence of amyloid
628 precursor protein (APP) by facilitating the transport of synaptic proteins and mitochondria (Shaw
629 and Chang, 2013). These conflicting results regarding the overexpression of *sra* demonstrate that
630 *sra* is involved with both APP and Aβ42 separate from its function of regulating calcineurin. It is
631 unclear if *sra* is working through calcineurin, APP, Aβ42 or other molecules to contribute to both
632 pre- and postsynaptic homeostatic signaling processes. This line of research may also lead to
633 examining other open questions such as how defective homeostatic synaptic processes may
634 contribute to neurodegeneration and other neural pathologies. It is known that most genes that are
635 necessary for PHP are linked to neural disorders and pathologies such as autism spectrum
636 disorders, schizophrenia, Fragile X Syndrome, migraine, and epilepsy (Wondolowski and Dickman,
637 2013, Frank et al., 2020).

638 Another idea for how the expression of *sra* may be regulating PHP is through its effects on
639 mitochondrial function. Both increases and decreases in *sra* have been shown to result in decreased
640 ATP levels, increased ROS production, decreased mitochondrial DNA in *Drosophila* heads,
641 decreased mitochondrial size, and increased mitochondrial number (Chang and Min, 2005). This is
642 independent from its function of regulating calcineurin as decreasing calcineurin activity in *sra*
643 mutants did not rescue mitochondrial enzymatic activity. Recent work also indicates that
644 Mitochondrial Complex I (MCI) is necessary for synapse function and plasticity at the *Drosophila*
645 NMJ (Mallik and Frank, 2022). Genetic knockdown or pharmacological inhibition of MCI impaired
646 neurotransmission, reduced NMJ growth and altered NMJ morphology.

647

648 **Acute versus chronic PHP expression with single tissue contributions**

649 There is strong evidence to suggest that there are shared mechanisms underlying both the acute
650 and chronic forms of PHP signaling as both forms display robust increases in readily releasable
651 pool (RRP) size and Ca_V2-mediated calcium influx that result in increases in quantal content
652 necessary for function PHP (Davis and Müller, 2015, Müller and Davis, 2012). Recent work has found
653 that the acute and chronic forms of PHP are functionally separable (James et al., 2019). Our data
654 support this idea by showing minimal overlap in a specific *sra* impairment in a specific tissue. For
655 example, *sra* knockdown postsynaptically only blocked acute PHP while leaving the chronic phase
656 intact; conversely, *sra* overexpression postsynaptically did not impair acute PHP while blocking
657 chronic PHP. These data demonstrate that *sra* is tightly regulated as both too much and too little
658 *sra* can disrupt PHP.

659 Our *CaNB* knockdown data also support the separation of the acute and chronic phases of
660 PHP as global knockdown led to a weak impairment in acute PHP while leaving chronic PHP
661 intact. Conversely, postsynaptic-specific knockdown led to a strong block in chronic PHP but left
662 acute PHP intact. These data support the separation of acute and chronic PHP as *sra* and *CaNB*
663 expression are likely regulating different processes at different timepoints that integrate to produce
664 functional PHP.

665 Other work has suggested that PHP pathways converge onto the same targets (Goel et al.,
666 2017). While it is possible that discrete signaling pathways converge, it is more likely that there is

667 some degree of convergence while also some amount of separate signaling systems. It will be
668 important for future studies to test how the individual influences of molecules from distinct
669 synaptic tissues underly the different phases of PHP to promote a fully functional PHP signaling
670 system. Collectively, our data indicate that some situations where PHP is blocked in the short run
671 are eventually resolved over developmental time if the synapse is given sufficient time to grow
672 and implement an array of compensatory mechanisms at its disposal (Goel et al., 2019). Conversely
673 there could be other situations where the synapse has a capacity for a quick response but fails to
674 respond after long periods of continuous challenge.

675

676 **Models of compensation: pharmacology vs. genetics, spatial vs. temporal**

677 The field of homeostatic synaptic plasticity faces a conundrum related to how PHP is
678 executed. Distinct acute pharmacological (PhTx) and chronic genetic manipulations (*GluRIIA*
679 loss) result in similar PHP expression mechanisms (Goel et al., 2017, Böhme et al., 2019, Müller et
680 al., 2012). Yet – depending upon the type of challenge used – important differences in PHP
681 expression have been observed. This has given rise to different models. Some groups have
682 proposed there exist differences in how the synapse executes PHP at phasic vs. tonic motor
683 terminals (Aponte-Santiago and Littleton, 2020, Genç and Davis, 2019, Newman et al., 2017, Sauvola et
684 al., 2021), depending upon pharamacological vs. genetic challenge. Recent characterization of
685 motor neuron-specific tools allow a refinement of analyses, at least in the context of presynaptic
686 terminals (Han et al., 2022, Aponte-Santiago et al., 2020, Wang et al., 2021). For a second model, a
687 recent study suggests that the type of pharmacological perturbation to glutamate receptors might
688 control the eventual response (Nair et al., 2021). A third model is that short-term and long-term
689 events that stabilize the NMJ are governed by genetically separable signaling systems (Brusich et
690 al., 2015, James et al., 2019, Spring et al., 2016, Yeates et al., 2017). This latter idea is analogous to
691 "early phase" and "late phase" events that trigger and consolidate Hebbian types of plasticity like
692 LTP (Bosch et al., 2014), and it gives rise to terms like "acute PHP" and "chronic PHP," similar to
693 what we have used here.

694 Importantly, these models are not mutually exclusive. Our data regarding calcineurin
695 regulation via Sarah is consistent with any of them. Intriguingly, misexpression of Sarah in the

postsynaptic muscle causes an increase in the levels of pCaMKII at boutons. By contrast, downregulation of pCaMKII has been shown by other groups to be a sentinel of successful PHP expression apposing type-Ib boutons, specifically when genetically impairing glutamate receptors (Li et al., 2018, Newman et al., 2017). Whether or not such a mechanistic difference is dictated strictly spatially or also temporally is yet to be full tested.

References

AHERN, G. P., JUNANKAR, P. R. & DULHUNTY, A. F. 1994. Single channel activity of the ryanodine receptor calcium release channel is modulated by FK-506. *FEBS Lett,* 352**,** 369-74.

ANDRE, E. A., FORCELLI, P. A. & PAK, D. T. 2018. What goes up must come down: homeostatic synaptic plasticity strategies in neurological disease. *Future Neurol,* 13**,** 13-21.

APONTE-SANTIAGO, N. A. & LITTLETON, J. T. 2020. Synaptic Properties and Plasticity Mechanisms of Invertebrate Tonic and Phasic Neurons. *Front Physiol,* 11**,** 611982.

APONTE-SANTIAGO, N. A., ORMEROD, K. G., AKBERGENOVA, Y. & LITTLETON, J. T. 2020. Synaptic Plasticity Induced by Differential Manipulation of Tonic and Phasic Motoneurons in Drosophila. *J Neurosci,* 40**,** 6270-6288.

BAUMGÄRTEL, K. & MANSUY, I. M. 2012. Neural functions of calcineurin in synaptic plasticity and memory. *Learn Mem,* 19**,** 375-84.

BETZ, H., SCHUSTER, C., ULTSCH, A. & SCHMITT, B. 1993. Molecular biology of ionotropic glutamate receptors in Drosophila melanogaster. *Trends in Pharmacological Sciences,* 14**,** 428-431.

BIENENSTOCK, E. L., COOPER, L. N. & MUNRO, P. W. 1982. Theory for the development of neuron selectivity: orientation specificity and binocular interaction in visual cortex. *J Neurosci,* 2**,** 32-48.

BLISS, T. V. P., COLLINGRIDGE, G. L. & MORRIS, R. G. M. 2014. Synaptic plasticity in health and disease: introduction and overview. *Philosophical Transactions of the Royal Society B: Biological Sciences,* 369**,** 20130129.

BÖHME, M. A., MCCARTHY, A. W., GRASSKAMP, A. T., BEUSCHEL, C. B., GOEL, P., JUSYTE, M., LABER, D., HUANG, S., REY, U., PETZOLDT, A. G., LEHMANN, M., GOTTFERT, F., HAGHIGHI, P., HELL, S. W., OWALD, D., DICKMAN, D., SIGRIST,

S. J. & WALTER, A. M. 2019. Rapid active zone remodeling consolidates presynaptic potentiation. *Nat Commun,* 10**,** 1085.

BOSCH, M., CASTRO, J., SANEYOSHI, T., MATSUNO, H., SUR, M. & HAYASHI, Y. 2014. Structural and molecular remodeling of dendritic spine substructures during long-term potentiation. *Neuron,* 82**,** 444-59.

BRUSICH, D. J., SPRING, A. M. & FRANK, C. A. 2015. A single-cross, RNA interference-based genetic tool for examining the long-term maintenance of homeostatic plasticity. *Front Cell Neurosci,* 9**,** 107.

BUDNIK, V., KOH, Y. H., GUAN, B., HARTMANN, B., HOUGH, C., WOODS, D. & GORCZYCA, M. 1996. Regulation of synapse structure and function by the Drosophila tumor suppressor gene dlg. *Neuron,* 17**,** 627-40.

BULTYNCK, G., DE SMET, P., WEIDEMA, A. F., VER HEYEN, M., MAES, K., CALLEWAERT, G., MISSIAEN, L., PARYS, J. B. & DE SMEDT, H. 2000. Effects of the immunosuppressant FK506 on intracellular Ca2+ release and Ca2+ accumulation mechanisms. *J Physiol,* 525 Pt 3**,** 681-93.

CESCA, F., BALDELLI, P., VALTORTA, F. & BENFENATI, F. 2010. The synapsins: key actors of synapse function and plasticity. *Prog Neurobiol,* 91**,** 313-48.

CHANG, K. T. & MIN, K. T. 2005. Drosophila melanogaster homolog of Down syndrome critical region 1 is critical for mitochondrial function. *Nat Neurosci,* 8**,** 1577-85.

CHANG, K. T., SHI, Y.-J. & MIN, K.-T. 2003. The Drosophila homolog of Down's syndrome critical region 1 gene regulates learning: Implications for mental retardation. *Proceedings of the National Academy of Sciences,* 100**,** 15794-15799.

CHI, P., GREENGARD, P. & RYAN, T. A. 2003. Synaptic vesicle mobilization is regulated by distinct synapsin I phosphorylation pathways at different frequencies. *Neuron,* 38**,** 69-78.

CLARDY, J. 1995. The chemistry of signal transduction. *Proceedings of the National Academy of Sciences of the United States of America,* 92**,** 56-61.

D'AMELIO, M., CAVALLUCCI, V., MIDDEI, S., MARCHETTI, C., PACIONI, S., FERRI, A., DIAMANTINI, A., DE ZIO, D., CARRARA, P., BATTISTINI, L., MORENO, S., BACCI, A., AMMASSARI-TEULE, M., MARIE, H. & CECCONI, F. 2011. Caspase-3 triggers early synaptic dysfunction in a mouse model of Alzheimer's disease. *Nat Neurosci,* 14**,** 69-76.

DAVIS, G. W. 2006. Homeostatic control of neural activity: from phenomenology to molecular design. *Annu Rev Neurosci,* 29**,** 307-23.

DAVIS, G. W., DIANTONIO, A., PETERSEN, S. A. & GOODMAN, C. S. 1998. Postsynaptic PKA controls quantal size and reveals a retrograde signal that regulates presynaptic transmitter release in Drosophila. *Neuron,* 20**,** 305-15.

765 DAVIS, G. W. & MÜLLER, M. 2015. Homeostatic control of presynaptic neurotransmitter
766 release. *Annu Rev Physiol,* 77**,** 251-70.

767 DEL CASTILLO, J. & KATZ, B. 1954. Quantal components of the end-plate potential. *J Physiol,*
768 124**,** 560-73.

769 DIANTONIO, A., PETERSEN, S. A., HECKMANN, M. & GOODMAN, C. S. 1999. Glutamate
770 receptor expression regulates quantal size and quantal content at the Drosophila
771 neuromuscular junction. *J Neurosci,* 19**,** 3023-32.

772 DICKMAN, D. & WONDOLOWSKI, J. 2013. Emerging links between homeostatic synaptic
773 plasticity and neurological disease. *Frontiers in Cellular Neuroscience,* 7.

774 FRANK, C. A. 2014a. Homeostatic plasticity at the Drosophila neuromuscular junction.
775 *Neuropharmacology,* 78**,** 63-74.

776 FRANK, C. A. 2014b. How voltage-gated calcium channels gate forms of homeostatic synaptic
777 plasticity. *Front Cell Neurosci,* 8**,** 40.

778 FRANK, C. A., JAMES, T. D. & MÜLLER, M. 2020. Homeostatic control of Drosophila
779 neuromuscular junction function. *Synapse,* 74**,** e22133.

780 FRANK, C. A., KENNEDY, M. J., GOOLD, C. P., MAREK, K. W. & DAVIS, G. W. 2006.
781 Mechanisms underlying the rapid induction and sustained expression of synaptic
782 homeostasis. *Neuron,* 52**,** 663-77.

783 FRANK, C. A., PIELAGE, J. & DAVIS, G. W. 2009. A presynaptic homeostatic signaling system
784 composed of the Eph receptor, ephexin, Cdc42, and CaV2.1 calcium channels. *Neuron,* 61**,**
785 556-69.

786 FURMAN, J. L. & NORRIS, C. M. 2014. Calcineurin and glial signaling: neuroinflammation and
787 beyond. *J Neuroinflammation,* 11**,** 158.

788 GAYDUKOV, A., TARASOVA, E. & BALEZINA, O. 2013. Calcium-dependent phosphatase
789 calcineurin downregulates evoked neurotransmitter release in neuromuscular junctions of
790 mice. *Neurochemical Journal,* 7**,** 29-33.

791 GENÇ, O. & DAVIS, G. W. 2019. Target-wide Induction and Synapse Type-Specific Robustness
792 of Presynaptic Homeostasis. *Curr Biol,* 29**,** 3863-3873 e2.

793 GOEL, P. & DICKMAN, D. 2018. Distinct homeostatic modulations stabilize reduced
794 postsynaptic receptivity in response to presynaptic DLK signaling. *Nat Commun,* 9**,** 1856.

795 GOEL, P., KHAN, M., HOWARD, S., KIM, G., KIRAGASI, B., KIKUMA, K. & DICKMAN,
796 D. 2019. A screen for synaptic growth mutants reveals mechanisms that stabilize synaptic
797 strength. *J Neurosci*.

GOEL, P., LI, X. & DICKMAN, D. 2017. Disparate Postsynaptic Induction Mechanisms Ultimately Converge to Drive the Retrograde Enhancement of Presynaptic Efficacy. *Cell Rep,* 21**,** 2339-2347.

GREENSPAN, R. J. 2004. *Fly pushing : the theory and practice of Drosophila genetics,* Cold Spring Harbor, N.Y., Cold Spring Harbor Laboratory Press.

HAN, Y., CHIEN, C., GOEL, P., HE, K., PINALES, C., BUSER, C. & DICKMAN, D. 2022. Botulinum neurotoxin accurately separates tonic vs. phasic transmission and reveals heterosynaptic plasticity rules in Drosophila. *Elife,* 11.

HARRIS, C. D., ERMAK, G. & DAVIES, K. J. 2005. Multiple roles of the DSCR1 (Adapt78 or RCAN1) gene and its protein product calcipressin 1 (or RCAN1) in disease. *Cell Mol Life Sci,* 62**,** 2477-86.

HARRIS, N., BRAISER, D. J., DICKMAN, D. K., FETTER, R. D., TONG, A. & DAVIS, G. W. 2015. The Innate Immune Receptor PGRP-LC Controls Presynaptic Homeostatic Plasticity. *Neuron,* 88**,** 1157-64.

HAZELRIGG, T., LEVIS, R. & RUBIN, G. M. 1984. Transformation of white locus DNA in drosophila: dosage compensation, zeste interaction, and position effects. *Cell,* 36**,** 469-81.

HE, K., SONG, L., CUMMINGS, L. W., GOLDMAN, J., HUGANIR, R. L. & LEE, H.-K. 2009. Stabilization of Ca²⁺-permeable AMPA receptors at perisynaptic sites by GluR1-S845 phosphorylation. *Proceedings of the National Academy of Sciences,* 106**,** 20033-20038.

HORNER, V. L., CZANK, A., JANG, J. K., SINGH, N., WILLIAMS, B. C., PURO, J., KUBLI, E., HANES, S. D., MCKIM, K. S., WOLFNER, M. F. & GOLDBERG, M. L. 2006. The Drosophila Calcipressin Sarah Is Required for Several Aspects of Egg Activation. *Current Biology,* 16**,** 1441-1446.

JAMES, T. D., ZWIEFELHOFER, D. J. & FRANK, C. A. 2019. Maintenance of homeostatic plasticity at the Drosophila neuromuscular synapse requires continuous IP3-directed signaling. *eLife,* 8.

JAN, L. Y. & JAN, Y. N. 1976. Properties of the larval neuromuscular junction in Drosophila melanogaster. *J Physiol,* 262**,** 189-214.

JOVANOVIC, J. N., SIHRA, T. S., NAIRN, A. C., HEMMINGS, H. C., JR., GREENGARD, P. & CZERNIK, A. J. 2001. Opposing changes in phosphorylation of specific sites in synapsin I during Ca2+-dependent glutamate release in isolated nerve terminals. *J Neurosci,* 21**,** 7944-53.

KADAMUR, G. & ROSS, E. M. 2013. Mammalian phospholipase C. *Annu Rev Physiol,* 75**,** 127-54.

833 KIKUMA, K., LI, X., PERRY, S., LI, Q., GOEL, P., CHEN, C., KIM, D., STAVROPOULOS, N.
834 & DICKMAN, D. 2019. Cul3 and insomniac are required for rapid ubiquitination of
835 postsynaptic targets and retrograde homeostatic signaling. *Nat Commun,* 10**,** 2998.

836 KINGSBURY, T. J. & CUNNINGHAM, K. W. 2000. A conserved family of calcineurin
837 regulators. *Genes & development,* 14**,** 1595-1604.

838 KOH, Y. H., POPOVA, E., THOMAS, U., GRIFFITH, L. C. & BUDNIK, V. 1999. Regulation of
839 DLG Localization at Synapses by CaMKII-Dependent Phosphorylation. *Cell,* 98**,** 353-363.

840 KOLES, K., MESSELAAR, E. M., FEIGER, Z., YU, C. J., FRANK, C. A. & RODAL, A. A.
841 2015. The EHD protein Past1 controls postsynaptic membrane elaboration and synaptic
842 function. *Molecular Biology of the Cell,* 26**,** 3275-3288.

843 KRICK, N., RYGLEWSKI, S., PICHLER, A., BIKBAEV, A., GÖTZ, T., KOBLER, O., HEINE,
844 M., THOMAS, U. & DUCH, C. 2021. Separation of presynaptic Ca_v2 and Ca_v1 channel
845 function in synaptic vesicle exo- and endocytosis by the membrane anchored Ca^{2+} pump
846 PMCA. *Proceedings of the National Academy of Sciences,* 118**,** e2106621118.

847 KUMASHIRO, S., LU, Y. F., TOMIZAWA, K., MATSUSHITA, M., WEI, F. Y. & MATSUI, H.
848 2005. Regulation of synaptic vesicle recycling by calcineurin in different vesicle pools.
849 *Neurosci Res,* 51**,** 435-43.

850 KUROMI, H., YOSHIHARA, M. & KIDOKORO, Y. 1997. An inhibitory role of calcineurin in
851 endocytosis of synaptic vesicles at nerve terminals of Drosophila larvae. *Neurosci Res,* 27**,**
852 101-13.

853 LEE, J. I., DHAKAL, B. K., LEE, J., BANDYOPADHYAY, J., JEONG, S. Y., EOM, S. H., KIM,
854 D. H. & AHNN, J. 2003. The Caenorhabditis elegans Homologue of Down Syndrome
855 Critical Region 1, RCN-1, Inhibits Multiple Functions of the Phosphatase Calcineurin.
856 *Journal of Molecular Biology,* 328**,** 147-156.

857 LEE, S., BANG, S. M., HONG, Y. K., LEE, J. H., JEONG, H., PARK, S. H., LIU, Q. F., LEE, I.
858 S. & CHO, K. S. 2016. The calcineurin inhibitor Sarah (Nebula) exacerbates Abeta42
859 phenotypes in a Drosophila model of Alzheimer's disease. *Dis Model Mech,* 9**,** 295-306.

860 LI, X., GOEL, P., CHEN, C., ANGAJALA, V., CHEN, X. & DICKMAN, D. K. 2018. Synapse-
861 specific and compartmentalized expression of presynaptic homeostatic potentiation. *Elife,*
862 7.

863 LIN, D. M. & GOODMAN, C. S. 1994. Ectopic and increased expression of Fasciclin II alters
864 motoneuron growth cone guidance. *Neuron,* 13**,** 507-23.

865 LIN, J. W., JU, W., FOSTER, K., LEE, S. H., AHMADIAN, G., WYSZYNSKI, M., WANG, Y.
866 T. & SHENG, M. 2000. Distinct molecular mechanisms and divergent endocytotic
867 pathways of AMPA receptor internalization. *Nat Neurosci,* 3**,** 1282-90.

868 LIU, J., FARMER, J. D., JR., LANE, W. S., FRIEDMAN, J., WEISSMAN, I. & SCHREIBER, S.
869 L. 1991. Calcineurin is a common target of cyclophilin-cyclosporin A and FKBP-FK506
870 complexes. *Cell,* 66**,** 807-15.

871 LLORET, A., BADIA, M. C., GIRALDO, E., ERMAK, G., ALONSO, M. D., PALLARDÓ, F.
872 V., DAVIES, K. J. & VIÑA, J. 2011. Amyloid-β toxicity and tau hyperphosphorylation
873 are linked via RCAN1 in Alzheimer's disease. *J Alzheimers Dis,* 27**,** 701-9.

874 MALLIK, B. & FRANK, C. A. 2022. Roles for Mitochondrial Complex I Subunits in Regulating
875 Synaptic Transmission and Growth. *Frontiers in Neuroscience,* 16.

876 MARDER, E. 2012. Neuromodulation of neuronal circuits: back to the future. *Neuron,* 76**,** 1-11.

877 MARRUS, S. B., PORTMAN, S. L., ALLEN, M. J., MOFFAT, K. G. & DIANTONIO, A. 2004.
878 Differential Localization of Glutamate Receptor Subunits at the Drosophila
879 Neuromuscular Junction. *The Journal of Neuroscience,* 24**,** 1406.

880 MCLACHLAN, E. M. & MARTIN, A. R. 1981. Non-linear summation of end-plate potentials in
881 the frog and mouse. *J Physiol,* 311**,** 307-24.

882 MENON, K. P., CARRILLO, R. A. & ZINN, K. 2013. Development and plasticity of the
883 Drosophila larval neuromuscular junction. *Wiley Interdiscip Rev Dev Biol,* 2**,** 647-70.

884 MÜLLER, M. & DAVIS, G. W. 2012. Transsynaptic control of presynaptic Ca^{2+} influx achieves
885 homeostatic potentiation of neurotransmitter release. *Current biology : CB,* 22**,** 1102-1108.

886 MÜLLER, M., GENÇ, Ö. & DAVIS, G. W. 2015. RIM-Binding Protein Links Synaptic
887 Homeostasis to the Stabilization and Replenishment of High Release Probability Vesicles.
888 *Neuron*.

889 MÜLLER, M., LIU, K. S., SIGRIST, S. J. & DAVIS, G. W. 2012. RIM Controls Homeostatic Plasticity
890 through Modulation of the Readily-Releasable Vesicle Pool. *J Neurosci,* 32**,** 16574-85.

891 MUSSON, R. E. & SMIT, N. P. 2011. Regulatory mechanisms of calcineurin phosphatase activity.
892 *Curr Med Chem,* 18**,** 301-15.

893 NAIR, A. G., MUTTATHUKUNNEL, P. & MÜLLER, M. 2021. Distinct molecular pathways
894 govern presynaptic homeostatic plasticity. *Cell Rep,* 37**,** 110105.

895 NAKAI, Y., HORIUCHI, J., TSUDA, M., TAKEO, S., AKAHORI, S., MATSUO, T., KUME, K.
896 & AIGAKI, T. 2011. Calcineurin and its regulator sra/DSCR1 are essential for sleep in
897 Drosophila. *J Neurosci,* 31**,** 12759-66.

898 NEWMAN, Z. L., HOAGLAND, A., AGHI, K., WORDEN, K., LEVY, S. L., SON, J. H., LEE,
899 L. P. & ISACOFF, E. Y. 2017. Input-Specific Plasticity and Homeostasis at the Drosophila
900 Larval Neuromuscular Junction. *Neuron,* 93**,** 1388-1404 e10.

901 PARK, J., OH, Y. & CHUNG, K. C. 2009. Two key genes closely implicated with the
902 neuropathological characteristics in Down syndrome: DYRK1A and RCAN1. *BMB Rep,*
903 42**,** 6-15.

904 PETERSEN, S. A., FETTER, R. D., NOORDERMEER, J. N., GOODMAN, C. S. &
905 DIANTONIO, A. 1997. Genetic analysis of glutamate receptors in Drosophila reveals a
906 retrograde signal regulating presynaptic transmitter release. *Neuron,* 19**,** 1237-48.

907 PHILIP, F., KADAMUR, G., SILOS, R. G., WOODSON, J. & ROSS, E. M. 2010. Synergistic
908 activation of phospholipase C-beta3 by Galpha(q) and Gbetagamma describes a simple
909 two-state coincidence detector. *Curr Biol,* 20**,** 1327-35.

910 POZO, K. & GODA, Y. 2010. Unraveling mechanisms of homeostatic synaptic plasticity. *Neuron,*
911 66**,** 337-51.

912 RUSNAK, F. & MERTZ, P. 2000. Calcineurin: form and function. *Physiol Rev,* 80**,** 1483-521.

913 SAUVOLA, C. W., AKBERGENOVA, Y., CUNNINGHAM, K. L., APONTE-SANTIAGO, N.
914 A. & LITTLETON, J. T. 2021. The decoy SNARE Tomosyn sets tonic versus phasic
915 release properties and is required for homeostatic synaptic plasticity. *Elife,* 10.

916 SHAW, J. L. & CHANG, K. T. 2013. Nebula/DSCR1 Upregulation Delays Neurodegeneration
917 and Protects against APP-Induced Axonal Transport Defects by Restoring Calcineurin and
918 GSK-3β Signaling. *PLOS Genetics,* 9**,** e1003792.

919 SIGAL, N. H. & DUMONT, F. J. 1992. Cyclosporin A, FK-506, and rapamycin: pharmacologic
920 probes of lymphocyte signal transduction. *Annu Rev Immunol,* 10**,** 519-60.

921 SIM, A. T., BALDWIN, M. L., ROSTAS, J. A., HOLST, J. & LUDOWYKE, R. I. 2003. The role
922 of serine/threonine protein phosphatases in exocytosis. *Biochem J,* 373**,** 641-59.

923 SPRING, A. M., BRUSICH, D. J. & FRANK, C. A. 2016. C-terminal Src Kinase Gates
924 Homeostatic Synaptic Plasticity and Regulates Fasciclin II Expression at the Drosophila
925 Neuromuscular Junction. *PLoS Genet,* 12**,** e1005886.

926 STEWART, B., ATWOOD, H., RENGER, J., WANG, J. & WU, C. 1994. Improved stability of
927 Drosophila larval neuromuscular preparations in haemolymph-like physiological solutions
928 A Neuroethology, sensory, neural, and behavioral physiology.

929 SWANSON, S. K., BORN, T., ZYDOWSKY, L. D., CHO, H., CHANG, H. Y., WALSH, C. T.
930 & RUSNAK, F. 1992. Cyclosporin-mediated inhibition of bovine calcineurin by
931 cyclophilins A and B. *Proc Natl Acad Sci U S A,* 89**,** 3741-5.

932 TAKEO, S., SWANSON, S. K., NANDANAN, K., NAKAI, Y., AIGAKI, T., WASHBURN, M.
933 P., FLORENS, L. & HAWLEY, R. S. 2012. Shaggy/glycogen synthase kinase 3beta and
934 phosphorylation of Sarah/regulator of calcineurin are essential for completion of
935 Drosophila female meiosis. *Proc Natl Acad Sci U S A,* 109**,** 6382-9.

936 TAKEO, S., TSUDA, M., AKAHORI, S., MATSUO, T. & AIGAKI, T. 2006. The Calcineurin
937 Regulator Sra Plays an Essential Role in Female Meiosis in Drosophila. *Current Biology,*
938 16**,** 1435-1440.

939 TARASOVA, E. O., GAYDUKOV, A. E. & BALEZINA, O. P. 2018. Calcineurin and Its Role in
940 Synaptic Transmission. *Biochemistry (Mosc),* 83**,** 674-689.

941 TOMITA, J., MITSUYOSHI, M., UENO, T., ASO, Y., TANIMOTO, H., NAKAI, Y., AIGAKI,
942 T., KUME, S. & KUME, K. 2011. Pan-Neuronal Knockdown of Calcineurin Reduces
943 Sleep in the Fruit Fly, Drosophila melanogaster. *The Journal of Neuroscience,*
944 31**,** 13137-13146.

945 TONONI, G. & CIRELLI, C. 2006. Sleep function and synaptic homeostasis. *Sleep Medicine*
946 *Reviews,* 10**,** 49-62.

947 VICTOR, R. G., THOMAS, G. D., MARBAN, E. & O'ROURKE, B. 1995. Presynaptic
948 modulation of cortical synaptic activity by calcineurin. *Proceedings of the National*
949 *Academy of Sciences of the United States of America,* 92**,** 6269-6273.

950 VONHOFF, F. & KESHISHIAN, H. 2017. In Vivo Calcium Signaling during Synaptic
951 Refinement at the Drosophila Neuromuscular Junction. *The Journal of Neuroscience,* 37**,**
952 5511-5526.

953 WANG, T., HAUSWIRTH, A. G., TONG, A., DICKMAN, D. K. & DAVIS, G. W. 2014.
954 Endostatin Is a Trans-Synaptic Signal for Homeostatic Synaptic Plasticity. *Neuron,* 83**,**
955 616-629.

956 WANG, Y., LOBB-RABE, M., ASHLEY, J., ANAND, V. & CARRILLO, R. A. 2021. Structural
957 and Functional Synaptic Plasticity Induced by Convergent Synapse Loss in the Drosophila
958 Neuromuscular Circuit. *J Neurosci,* 41**,** 1401-1417.

959 WEN, Z., GUIRLAND, C., MING, G. L. & ZHENG, J. Q. 2004. A CaMKII/calcineurin switch
960 controls the direction of Ca(2+)-dependent growth cone guidance. *Neuron,* 43**,** 835-46.

961 WEYHERSMÜLLER, A., HALLERMANN, S., WAGNER, N. & EILERS, J. 2011. Rapid active zone
962 remodeling during synaptic plasticity. *J Neurosci,* 31**,** 6041-52.

963 WONDOLOWSKI, J. & DICKMAN, D. 2013. Emerging links between homeostatic synaptic
964 plasticity and neurological disease. *Front Cell Neurosci,* 7**,** 223.

965 WU, X.-S., ZHANG, Z., ZHAO, W.-D., WANG, D., LUO, F. & WU, L.-G. 2014. Calcineurin is
966 universally involved in vesicle endocytosis at neuronal and nonneuronal secretory cells.
967 *Cell reports,* 7**,** 982-988.

968 YAKEL, J. L. 1997. Calcineurin regulation of synaptic function: from ion channels to transmitter
969 release and gene transcription. *Trends Pharmacol Sci,* 18**,** 124-34.

970 YEATES, C. J. & FRANK, C. A. 2021. Homeostatic Depression Shows Heightened Sensitivity to
971 Synaptic Calcium. *Front Cell Neurosci,* 15**,** 618393.

972 YEATES, C. J., ZWIEFELHOFER, D. J. & FRANK, C. A. 2017. The Maintenance of Synaptic
973 Homeostasis at the Drosophila Neuromuscular Junction Is Reversible and Sensitive to
974 High Temperature. *eNeuro,* 4.

975 YOUNGER, M. A., MÜLLER, M., TONG, A., PYM, E. C. & DAVIS, G. W. 2013. A presynaptic
976 ENaC channel drives homeostatic plasticity. *Neuron,* 79**,** 1183-96.

977 ZHAO, J.-W., GAO, Z.-L., ZHANG, H.-Y., JI, Q.-Y., WANG, H., YANG, Y.-D., XING, F.-J.,
978 MENG, L.-J. & WANG, Y. 2012. Regulation of Cofilin Activity by CaMKII and
979 Calcineurin. *The American Journal of the Medical Sciences,* 344**,** 462-472.

980

981

982 **Figure 1.** Dual pre and postsynaptic knockdown or overexpression of *sra* does not block PHP **(A-**
983 **C)** Quantification showing average mEPSP amplitude, EPSP amplitude, and NLS quantal content
984 in pre + post-GAL4 control and pre + post-GAL4 driven *sra RNAi*. Black points show DMSO
985 control synapses, green points show synapses treated with PhTx, and magenta points show animals
986 chronically challenged with *GluRIII RNAi*. **(D, H)** Representative electrophysiological traces of
987 EPSPs (above) and mEPSPs (below). Scale bars for all traces are y = 10 mV (1mV), x = 20 ms
988 (500 ms) for EPSPs (mEPSPs). **(E-G)** Quantification showing average mEPSP amplitude, EPSP
989 amplitude, and NLS quantal content in pre + post-GAL4 control and pre + post-GAL4 driven *sra*
990 overexpression (OE). Black points show DMSO control synapses, green points show synapses
991 treated with PhTx, and magenta points show animals chronically challenged with *GluRIII RNAi*.
992 $*p<0.05$, $**p<0.01$, $***p<0.001$ by Multiple Student's T-test and corrected for multiple
993 comparisons using the Holm-Sidak method. DMSO controls were compared to PhTx and *GluRIII*
994 *RNAi* synapses for driver controls and separately for *sra RNAi* or OE.

995

996 **Figure 2.** Global *sra* mutation does not preclude PHP but does show an evoked amplitude decrease
997 in low calcium conditions. **(A-C)** Quantification showing average mEPSP, EPSP amplitude, and
998 NLS quantal content in $sra^{Mi06345}$, $sra^{Mi06345}/Df(3R)sbd^{104}$, and $GluRIIA^{SP16}$;
999 $sra^{Mi06345}/Df(3R)sbd^{104}$. **(D, H)** Representative electrophysiological traces of EPSPs (above) and
1000 mEPSPs (below). Scale bars for all traces are y = 10 mV (1mV), x = 20 ms (500 ms) for EPSPs
1001 (mEPSPs). **(E-G)** Experiments conducted in low calcium (0.2mM). Quantification showing
1002 average mEPSP, EPSP amplitude, and NLS quantal content in $sra^{Mi06345}$, $sra^{Mi06345}/Df(3R)sbd^{104}$,
1003 and $GluRIIA^{SP16}$; $sra^{Mi06345}/Df(3R)sbd^{104}$. Ordinary one-way ANOVAs were used to compare each
1004 genotype followed by a Tukey's HSD test for multiple comparisons. $*p<0.05$, $**p<0.01$,
1005 $***p<0.001$.

1006

1007 **Figure 3.** Acute expression of presynaptic homeostatic potentiation requires muscle expression of
1008 *sra*, but maintenance does not. **(A-C)** Quantification showing average mEPSP amplitude, EPSP
1009 amplitude, and NLS quantal content in post-GAL4 control and post-GAL4 driven *sra* RNAi. Black
1010 points show DMSO control synapses, while green points show synapses treated with PhTx. **(D, H)**
1011 Representative electrophysiological traces of EPSPs (above) and mEPSPs (below). Scale bars for

1012 all traces are y = 10 mV (1mV), x = 20 ms (500 ms) for EPSPs (mEPSPs). **(E-G)** Quantification
1013 showing average mEPSP amplitude, EPSP amplitude, and NLS quantal content in post-GAL4
1014 control and post-GAL4 driven *sra* RNAi in both the presence and absence of $GluRIIA^{SP16}$.
1015 *p<0.05, **p<0.01, ***p<0.001 by Student's T-test versus non-challenged genetic control.

1016

1017 **Figure 4.** Maintenance of presynaptic homeostatic potentiation is impaired by muscle
1018 overexpression of *sra*, but acute expression is not. **(A-C)** Quantification showing average mEPSP
1019 amplitude, EPSP amplitude, and NLS quantal content in post-GAL4 control and post-GAL4 driven
1020 *sra* overexpression (OE). Black points show DMSO control synapses, while green points show
1021 synapses treated with PhTx. **(D, H)** Representative electrophysiological traces of EPSPs (above)
1022 and mEPSPs (below). Scale bars for all traces are y = 10 mV (1mV), x = 20 ms (500 ms) for EPSPs
1023 (mEPSPs). **(E-G)** Quantification showing average mEPSP amplitude, EPSP amplitude, and NLS
1024 quantal content in post-GAL4 control and post-GAL4 driven *sra* OE in both the presence and
1025 absence of $GluRIIA^{SP16}$. *p<0.05, **p<0.01, ***p<0.001 by Student's T-test versus non-
1026 challenged genetic control.

1027

1028 **Figure 5.** Postsynaptic *sra* overexpression does not impair synapse development. **(A-F)** NMJs
1029 were co-stained with anti-DLG (magenta) and anti-Synapsin antibodies (green) to visualize
1030 synaptic boutons. **(G)** NMJ growth was assessed by bouton counting at abdominal segments A2
1031 and A3, muscle 6/7, based on postsynaptic DLG staining and checking for presynaptic Synapsin.
1032 **(H)** Bouton counts were normalized per unit of muscle 6/7 area. Ordinary one-way ANOVAs were
1033 used to compare each genotype within each segment followed by a Tukey's HSD test for multiple
1034 comparisons. *p<0.05, **p<0.01, ***p<0.001.

1035

1036 **Figure 6.** Postsynaptic *sra* overexpression disrupts pCaMKII in Ib postsynaptic densities. **(A)**
1037 Maximum-intensity projections of pCaMKII (magenta) and GluRIII (green). Merged images of
1038 both channels shown in top row. Representative bouton maximum-intensity projections of
1039 pCaMKII (middle row) and GluRIII (bottom row) are shown as heat maps. **(B)** Quantification of
1040 pCaMKII intensity as a percentage relative to wild type boutons. Each point represents the

1041 intensity at an individual Ib postsynaptic density. **(C)** Quantification of GluRIII intensity as a
1042 percentage relative to wild type boutons. Ordinary one-way ANOVAs were used to compare each
1043 genotype followed by a Tukey's HSD test for multiple comparisons. *p<0.05, **p<0.01,
1044 ***p<0.001.

1045

1046 **Figure 7.** Maintenance of presynaptic homeostatic potentiation is impaired by neuronal
1047 knockdown of *sra*, but acute expression is not. **(A-C)** Quantification showing average mEPSP
1048 amplitude, EPSP amplitude, and NLS quantal content in pre-GAL4 control and pre-GAL4 driven
1049 *sra* RNAi. Black points show DMSO control synapses, while green points show synapses treated
1050 with PhTx. **(D, H)** Representative electrophysiological traces of EPSPs (above) and mEPSPs
1051 (below). Scale bars for all traces are y = 10 mV (1mV), x = 20 ms (500 ms) for EPSPs (mEPSPs).
1052 **(E-G)** Quantification showing average mEPSP amplitude, EPSP amplitude, and NLS quantal
1053 content in pre-GAL4 control and pre-GAL4 driven *sra* RNAi in both the presence and absence of
1054 $GluRIIA^{SP16}$. *p<0.05, **p<0.01, ***p<0.001 by Student's T-test versus non-challenged genetic
1055 control.

1056

1057 **Figure 8.** Maintenance of presynaptic homeostatic potentiation is impaired by neuronal
1058 overexpression of *sra*, but acute expression is not. **(A-C)** Quantification showing average mEPSP
1059 amplitude, EPSP amplitude, and NLS quantal content in pre-GAL4 control and pre-GAL4 driven
1060 *sra* overexpression (OE). Black points show DMSO control synapses, while green points show
1061 synapses treated with PhTx. **(D, H)** Representative electrophysiological traces of EPSPs (above)
1062 and mEPSPs (below). Scale bars for all traces are y = 10 mV (1mV), x = 20 ms (500 ms) for EPSPs
1063 (mEPSPs). **(E-G)** Quantification showing average mEPSP amplitude, EPSP amplitude, and NLS
1064 quantal content in pre-GAL4 control and pre-GAL4 driven *sra* OE in both the presence and
1065 absence of $GluRIIA^{SP16}$. *p<0.05, **p<0.01, ***p<0.001 by Student's T-test versus non-
1066 challenged genetic control.

1067

1068 **Figure 9.** Pharmacological inhibition of calcineurin partially rescues the PHP deficit observed in
1069 chronically challenged postsynaptic overexpression of *sra* animals. **(A-C)** Quantification showing

1070 average mEPSP amplitude, EPSP amplitude, and NLS quantal content in post-GAL4 control and
1071 post-GAL4 driven *sra* overexpression (OE) in both the presence and absence of 50µM FK506.
1072 Black points show DMSO control synapses while dark pink points represent 50µM FK506. **(D)**
1073 Representative electrophysiological traces of EPSPs (above) and mEPSPs (below). Scale bars for
1074 all traces are y = 10 mV (1mV), x = 20 ms (500 ms) for EPSPs (mEPSPs). Two-way ANOVAs
1075 were used to compare each genotype with and without drug followed by a Tukey's HSD test for
1076 multiple comparisons. *p<0.05, **p<0.01, ***p<0.001.

1077

1078 **Figure 10.** Pharmacological inhibition of calcineurin rescues the PHP deficit observed in
1079 chronically challenged presynaptic knockdown of *sra* animals. **(A-C)** Quantification showing
1080 average mEPSP amplitude, EPSP amplitude, and NLS quantal content in pre-GAL4 control and
1081 pre-GAL4 driven *sra* knockdown in both the presence and absence of 50µM FK506. Black points
1082 show DMSO control synapses while dark pink points represent 50µM FK506. **(D)** Representative
1083 electrophysiological traces of EPSPs (above) and mEPSPs (below). Scale bars for all traces are y
1084 = 10 mV (1mV), x = 20 ms (500 ms) for EPSPs (mEPSPs). Two-way ANOVAs were used to
1085 compare each genotype with and without drug followed by a Tukey's HSD test for multiple
1086 comparisons. *p<0.05, **p<0.01, ***p<0.001.

1087

1088 **Figure 11.** Maintenance of presynaptic homeostatic potentiation can be further potentiated by
1089 pharmacologically inhibiting calcineurin. **(A-D)** Quantification showing average mEPSP
1090 amplitude, EPSP amplitude, NLS quantal content, and mEPSP frequency in wild type and
1091 *GluRIIA*^{SP16} animals. Black points show 10µM DMSO control, light pink points show 10µM
1092 FK506, grey points show 50µM DMSO control, and dark pink points show 50µM FK506. **(E,F)**
1093 Quantification of failure analysis experiment. 0.10mM Ca^{2+} was used in this experiment. "%
1094 failures" represents the number of stimulation pulses that failed to elicit any discernable response
1095 out of the 100 total pulses per synapse. Black points represent DMSO control, while the dark pink
1096 points represent 50µM FK506. **(G-I)** Quantification showing average mEPSP amplitude, EPSP
1097 amplitude, and NLS quantal content in wild type and *GluRIIA*^{SP16} animals dissected in low calcium
1098 conditions (0.20mM Ca^{2+}). Black points represent DMSO control, while the dark pink points

represent 50µM FK506. *p<0.05, **p<0.01, ***p<0.001 by Student's T-test versus non-drugged control.

Figure 12. Dual pre- and postsynaptic knockdown of *CaNB* does not block PHP while knockdown in muscle alone precluded the maintenance of PHP **(A-C)** Quantification showing average mEPSP amplitude, EPSP amplitude, and NLS quantal content in pre + post-GAL4 control and pre + post-GAL4 driven *CaNB* RNAi. Black points show DMSO control synapses, green points show synapses treated with PhTx, and magenta points show animals chronically challenged with *GluRIII* RNAi. **(D)** Representative electrophysiological traces of EPSPs (above) and mEPSPs (below). Scale bars for all traces are y = 10 mV (1mV), x = 20 ms (500 ms) for EPSPs (mEPSPs). *p<0.05, **p<0.01, ***p<0.001 by Multiple Student's T-test and corrected for multiple comparisons using the Holm-Sidak method. DMSO controls were compared to PhTx and *GluRIII* RNAi synapses for driver controls and separately for *CaNB* RNAi.

Conflict of Interest

The authors declare that the research was conducted in the absence of any commercial or financial relationships that could be construed as a potential conflict of interest.

Author Contributions

NSA and CAF designed the research, analyzed the data, and wrote the manuscript. NSA performed the research. Both authors contributed to the article and approved the submitted version.

Funding

This work was supported by grants from the National Institutes of Health/NINDS (NS085164 and NS130108) to CAF. This work was also supported by NIN/NINDS grant supplement to NSA for grant NS085164 (PI - CAF). Additional funds supporting parts of this work have been provided

by the University of Iowa Carver College of Medicine (CCOM) and the PI's home department within CCOM, Anatomy and Cell Biology.

Acknowledgements

We thank members of the Frank lab for helpful comments throughout this study. We thank the laboratories of Tina Tootle, Toshihiro Kitamoto, Pamela Geyer, and Lori Wallrath for helpful discussions. Additionally, we thank Drs. Samuel Young, Joshua Weiner, and Catherine Marcinkiewcz for helpful suggestions. We also thank the Bloomington Drosophila Resource Stock Center for several fly stocks detailed in the Methods section.

Supplementary Material

Supplementary Tables S1-S4 and S7-S12 show raw electrophysiology data. Table S5 shows raw bouton counts and measurements for NMJ growth assessment. Table S6 shows raw pCaMKII and GluRIII intensity measurements.

Data Availability Statement

The raw datasets for this study will be made available by the authors.

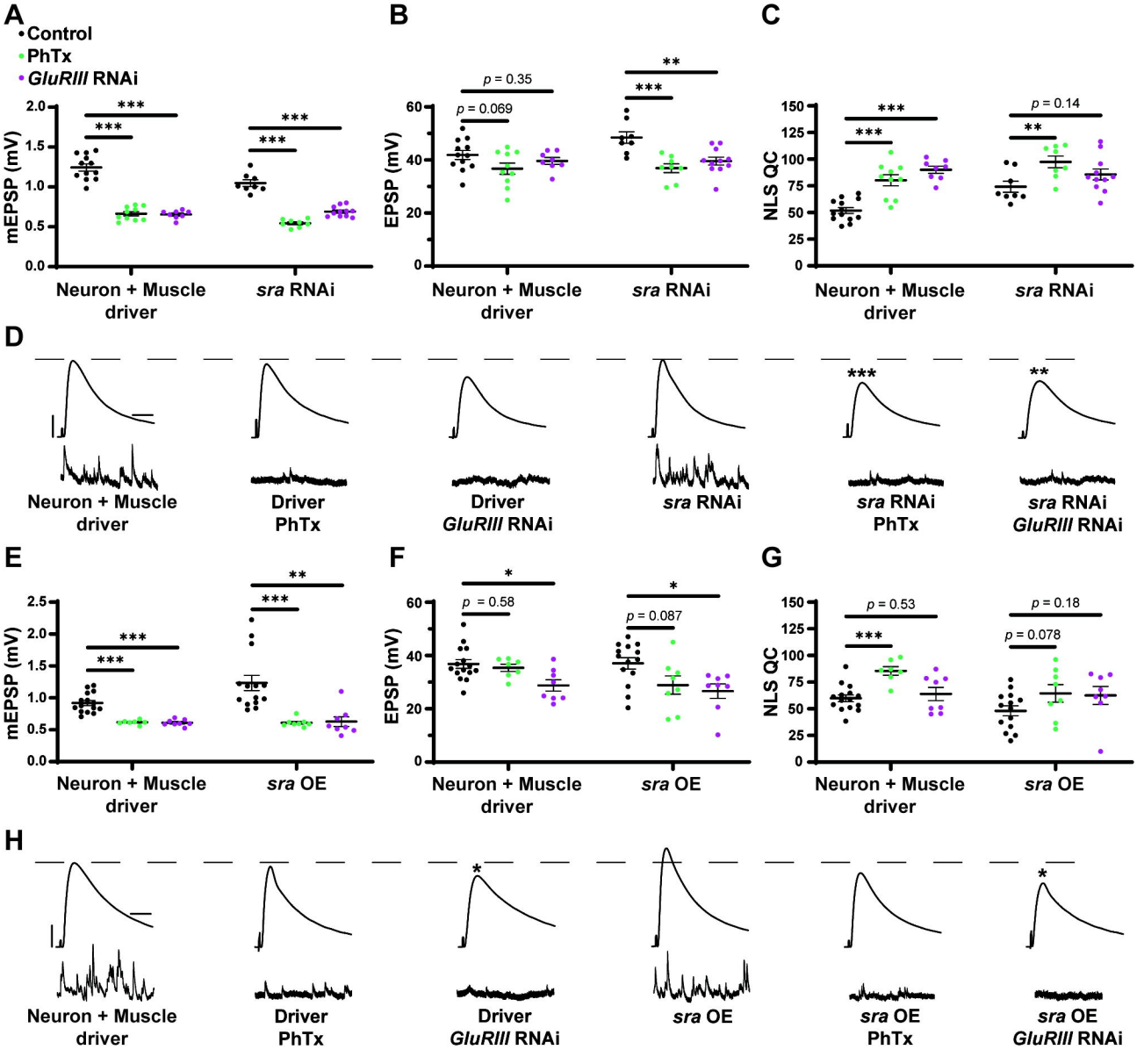
A
Control
PhTx
GluRIII RNAi
mEPSP (mV)
Neuron + Muscle driver
sra RNAi
B
EPSP (mV)
p = 0.35
p = 0.069
C
NLS QC
p = 0.14
D
Neuron + Muscle driver
Driver PhTx
Driver GluRIII RNAi
sra RNAi
sra RNAi PhTx
sra RNAi GluRIII RNAi
E
sra OE
F
p = 0.58
p = 0.087
G
p = 0.53
p = 0.078
H
Driver PhTx
Driver GluRIII RNAi
sra OE
sra OE PhTx
sra OE GluRIII RNAi

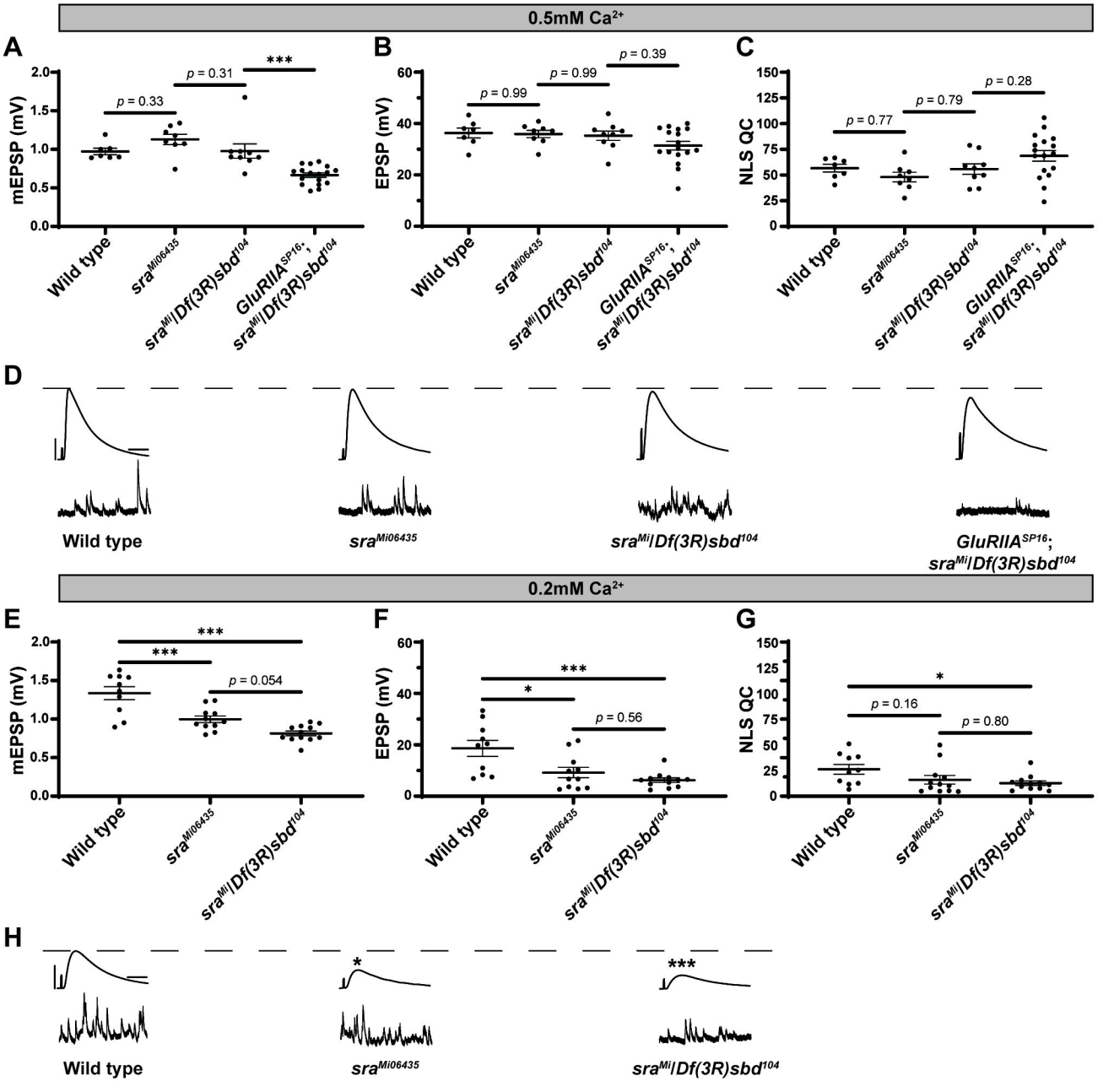
0.5mM Ca2+
A
mEPSP (mV)
p = 0.33
p = 0.31
***
Wild type
sraMi06435
sraMi/Df(3R)sbd104
GluRIIASP16; sraMi/Df(3R)sbd104
B
EPSP (mV)
p = 0.99
p = 0.99
p = 0.39
C
NLS QC
p = 0.77
p = 0.79
p = 0.28
D
Wild type
sraMi06435
sraMi/Df(3R)sbd104
GluRIIASP16; sraMi/Df(3R)sbd104
0.2mM Ca2+
E
mEPSP (mV)
***
***
p = 0.054
F
EPSP (mV)
***
*
p = 0.56
G
NLS QC
*
p = 0.16
p = 0.80
H
*
***
Wild type
sraMi06435
sraMi/Df(3R)sbd104

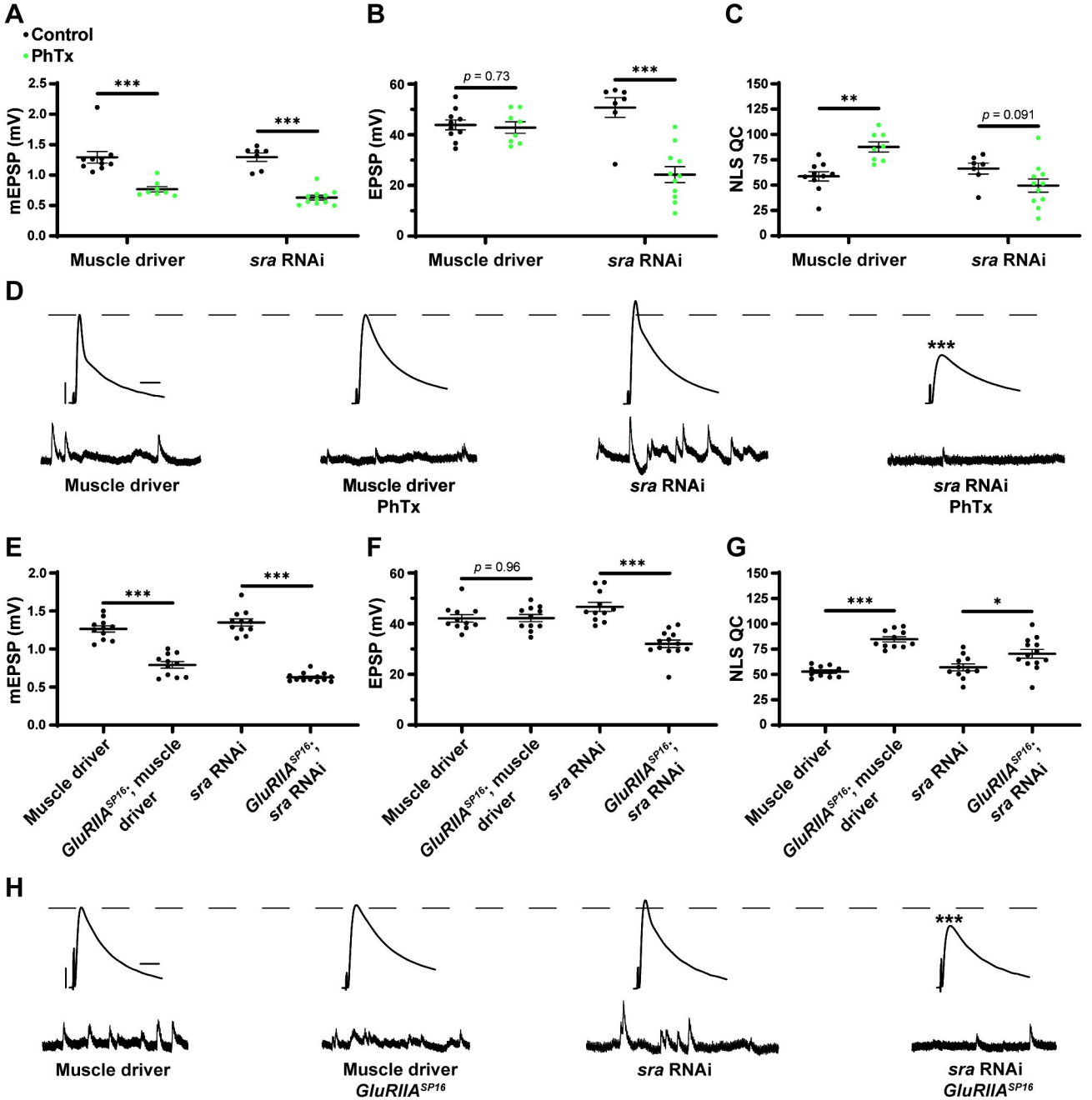
A
Control
PhTx
mEPSP (mV)
***
***
Muscle driver
sra RNAi
B
EPSP (mV)
p = 0.73
***
Muscle driver
sra RNAi
C
NLS QC
**
p = 0.091
Muscle driver
sra RNAi
D
***
Muscle driver
Muscle driver PhTx
sra RNAi
sra RNAi PhTx
E
mEPSP (mV)
***
***
Muscle driver
GluRIIA^SP16; muscle driver
sra RNAi
GluRIIA^SP16; sra RNAi
F
EPSP (mV)
p = 0.96
***
Muscle driver
GluRIIA^SP16; muscle driver
sra RNAi
GluRIIA^SP16; sra RNAi
G
NLS QC
***
*
Muscle driver
GluRIIA^SP16; muscle driver
sra RNAi
GluRIIA^SP16; sra RNAi
H
***
Muscle driver
Muscle driver GluRIIA^SP16
sra RNAi
sra RNAi GluRIIA^SP16

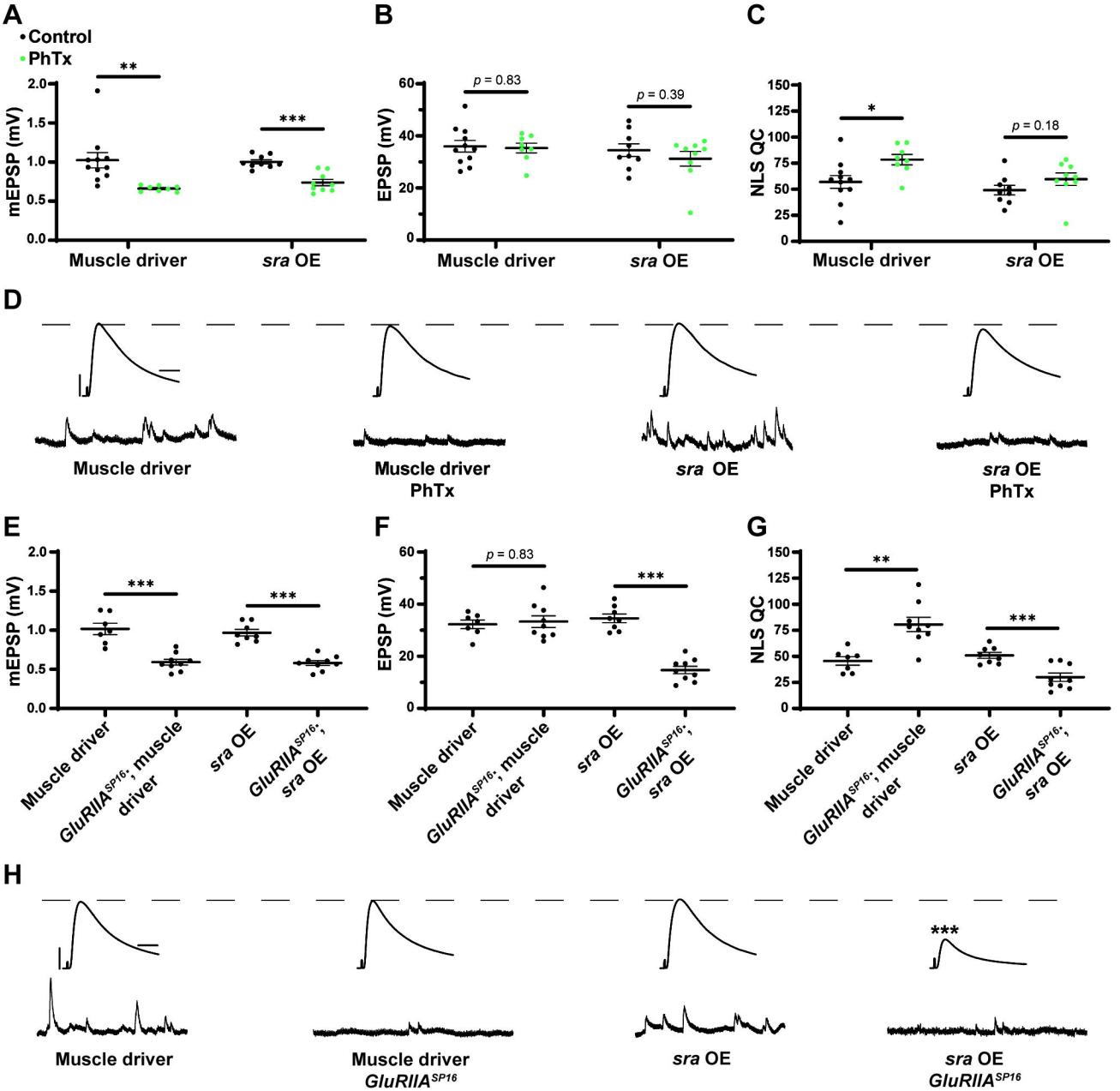
A
Control
PhTx
mEPSP (mV)
2.0
1.5
1.0
0.5
0.0
**
***
Muscle driver
sra OE
B
EPSP (mV)
60
40
20
0
p = 0.83
p = 0.39
Muscle driver
sra OE
C
NLS QC
150
125
100
75
50
25
0
*
p = 0.18
Muscle driver
sra OE
D
Muscle driver
Muscle driver PhTx
sra OE
sra OE PhTx
E
mEPSP (mV)
2.0
1.5
1.0
0.5
0.0
***
***
Muscle driver
GluRIIA^SP16; muscle driver
sra OE
GluRIIA^SP16; sra OE
F
EPSP (mV)
60
40
20
0
p = 0.83
***
Muscle driver
GluRIIA^SP16; muscle driver
sra OE
GluRIIA^SP16; sra OE
G
NLS QC
150
125
100
75
50
25
0
**
***
Muscle driver
GluRIIA^SP16; muscle driver
sra OE
GluRIIA^SP16; sra OE
H
***
Muscle driver
Muscle driver GluRIIA^SP16
sra OE
sra OE GluRIIA^SP16

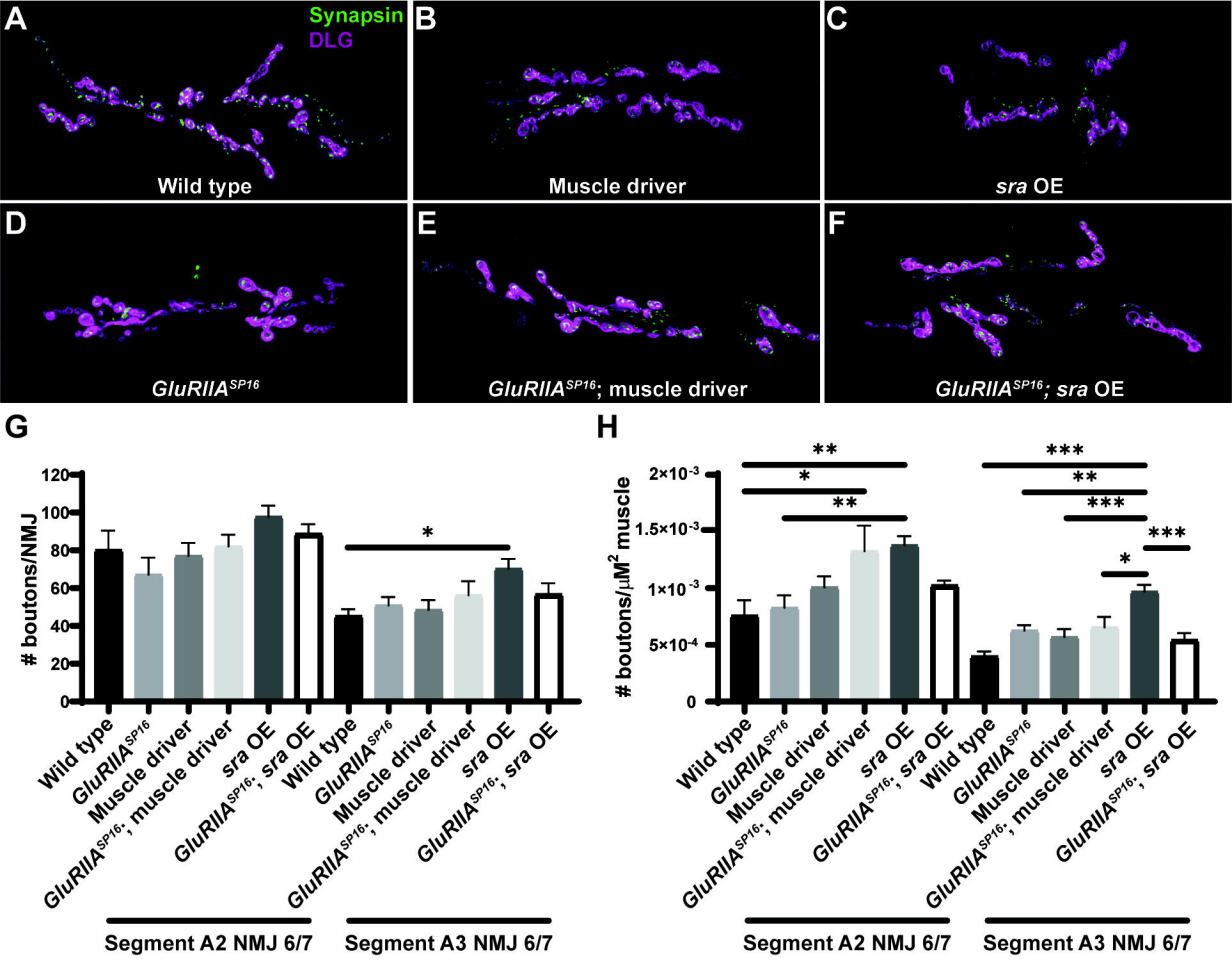
A
Synapsin
DLG
Wild type
B
Muscle driver
C
sra OE
D
GluRIIA^SP16
E
GluRIIA^SP16; muscle driver
F
GluRIIA^SP16; sra OE
G
boutons/NMJ
120
100
80
60
40
20
0
*
Wild type
GluRIIA^SP16
Muscle driver
GluRIIA^SP16; muscle driver
sra OE
GluRIIA^SP16; sra OE
Wild type
GluRIIA^SP16
Muscle driver
GluRIIA^SP16; muscle driver
sra OE
GluRIIA^SP16; sra OE
Segment A2 NMJ 6/7
Segment A3 NMJ 6/7
H
boutons/μM² muscle
2×10⁻³
1.5×10⁻³
1×10⁻³
5×10⁻⁴
0
**
*
**
***
**
***
*
***
Wild type
GluRIIA^SP16
Muscle driver
GluRIIA^SP16; muscle driver
sra OE
GluRIIA^SP16; sra OE
Wild type
GluRIIA^SP16
Muscle driver
GluRIIA^SP16; muscle driver
sra OE
GluRIIA^SP16; sra OE
Segment A2 NMJ 6/7
Segment A3 NMJ 6/7

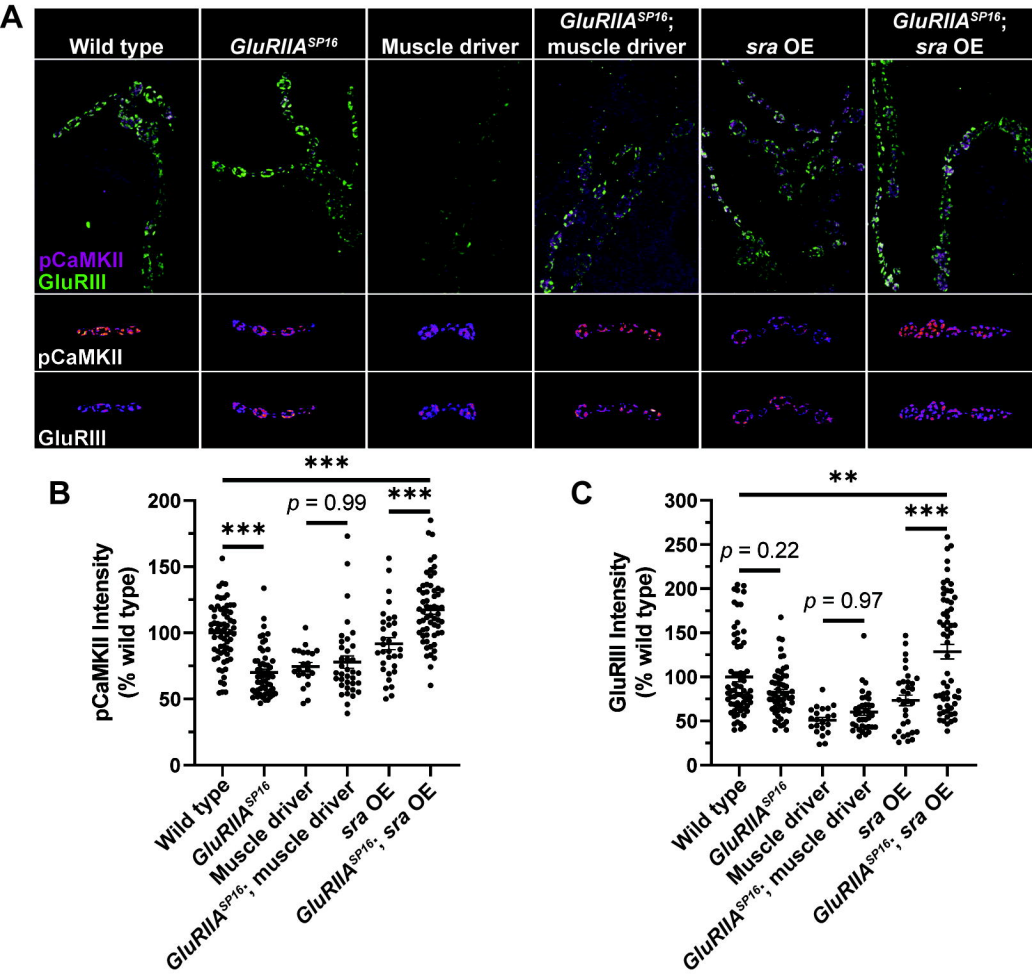
A
Wild type
GluRIIA^SP16
Muscle driver
GluRIIA^SP16; muscle driver
sra OE
GluRIIA^SP16; sra OE
pCaMKII
GluRIII
pCaMKII
GluRIII
B
pCaMKII Intensity (% wild type)
***
p = 0.99
***
***
C
GluRIII Intensity (% wild type)
**
p = 0.22
p = 0.97
***
Wild type
GluRIIA^SP16
Muscle driver
GluRIIA^SP16; muscle driver
sra OE
GluRIIA^SP16; sra OE

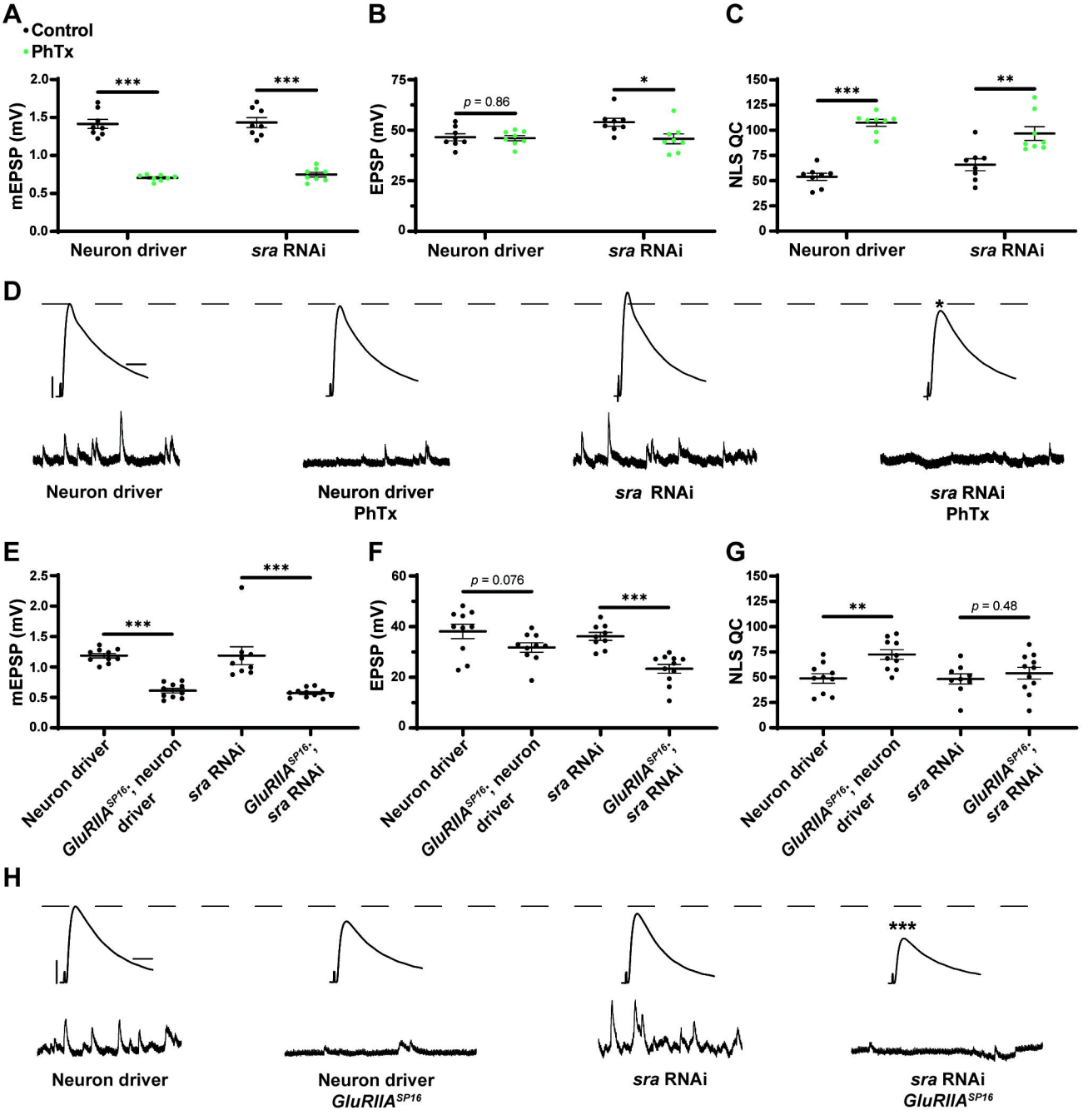
A
Control
PhTx
mEPSP (mV)
2.0
1.5
1.0
0.5
0.0
***
***
Neuron driver
sra RNAi
B
EPSP (mV)
75
50
25
0
p = 0.86
*
Neuron driver
sra RNAi
C
NLS QC
150
125
100
75
50
25
0
***
**
Neuron driver
sra RNAi
D
*
Neuron driver
Neuron driver PhTx
sra RNAi
sra RNAi PhTx
E
mEPSP (mV)
2.5
2.0
1.5
1.0
0.5
0.0
***
***
Neuron driver
GluRIIA^SP16; neuron driver
sra RNAi
GluRIIA^SP16; sra RNAi
F
EPSP (mV)
60
40
20
0
p = 0.076
***
Neuron driver
GluRIIA^SP16; neuron driver
sra RNAi
GluRIIA^SP16; sra RNAi
G
NLS QC
150
125
100
75
50
25
0
**
p = 0.48
Neuron driver
GluRIIA^SP16; neuron driver
sra RNAi
GluRIIA^SP16; sra RNAi
H
***
Neuron driver
Neuron driver GluRIIA^SP16
sra RNAi
sra RNAi GluRIIA^SP16

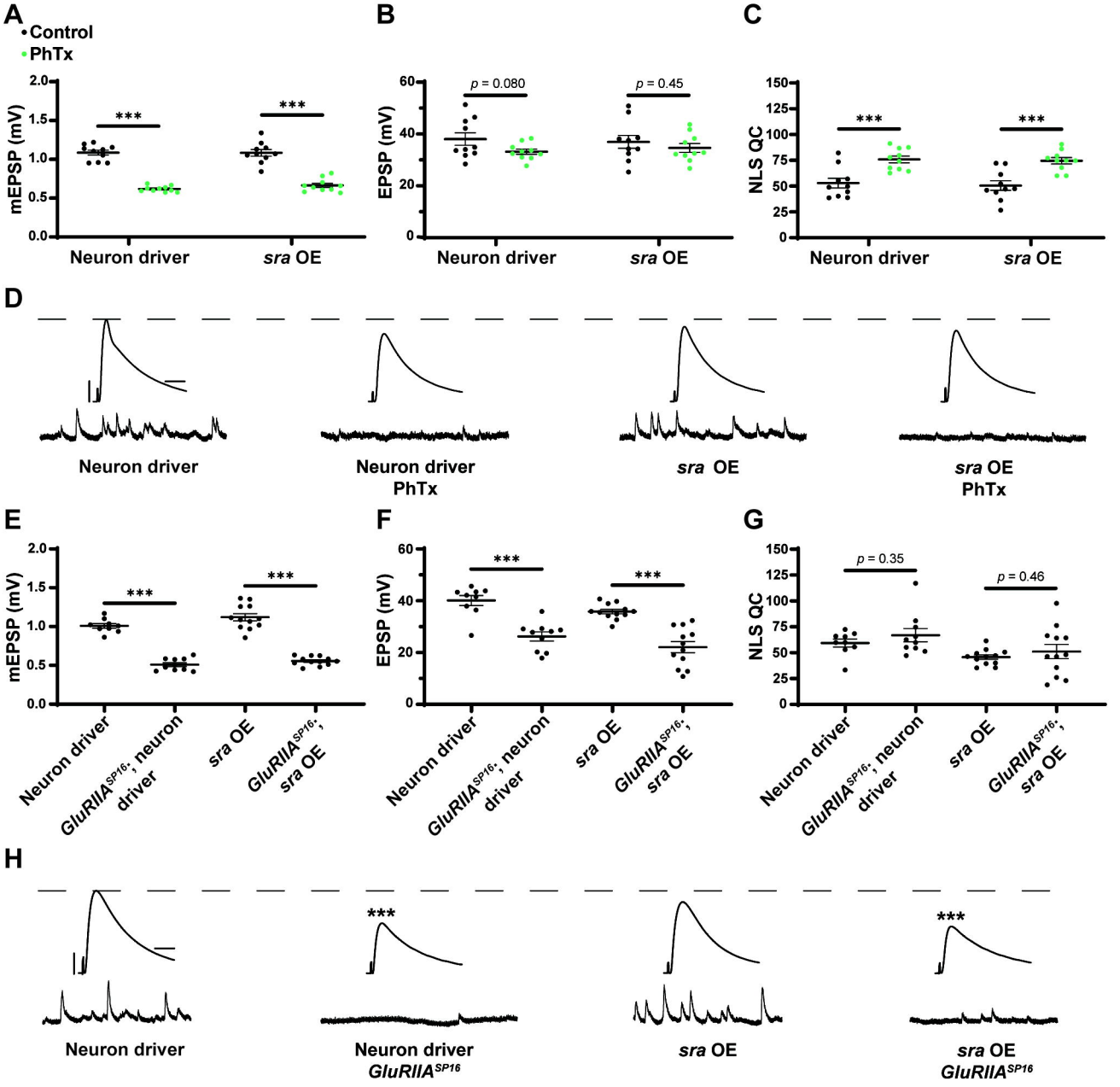
A
Control
PhTx
mEPSP (mV)
2.0
1.5
1.0
0.5
0.0
***
***
Neuron driver
sra OE
B
EPSP (mV)
60
40
20
0
p = 0.080
p = 0.45
Neuron driver
sra OE
C
NLS QC
150
125
100
75
50
25
0
***
***
Neuron driver
sra OE
D
Neuron driver
Neuron driver PhTx
sra OE
sra OE PhTx
E
mEPSP (mV)
2.0
1.5
1.0
0.5
0.0
***
***
Neuron driver
GluRIIA SP16, neuron driver
sra OE
GluRIIA SP16, sra OE
F
EPSP (mV)
60
40
20
0
***
***
Neuron driver
GluRIIA SP16, neuron driver
sra OE
GluRIIA SP16, sra OE
G
NLS QC
150
125
100
75
50
25
0
p = 0.35
p = 0.46
Neuron driver
GluRIIA SP16, neuron driver
sra OE
GluRIIA SP16, sra OE
H
***
***
Neuron driver
Neuron driver GluRIIA SP16
sra OE
sra OE GluRIIA SP16

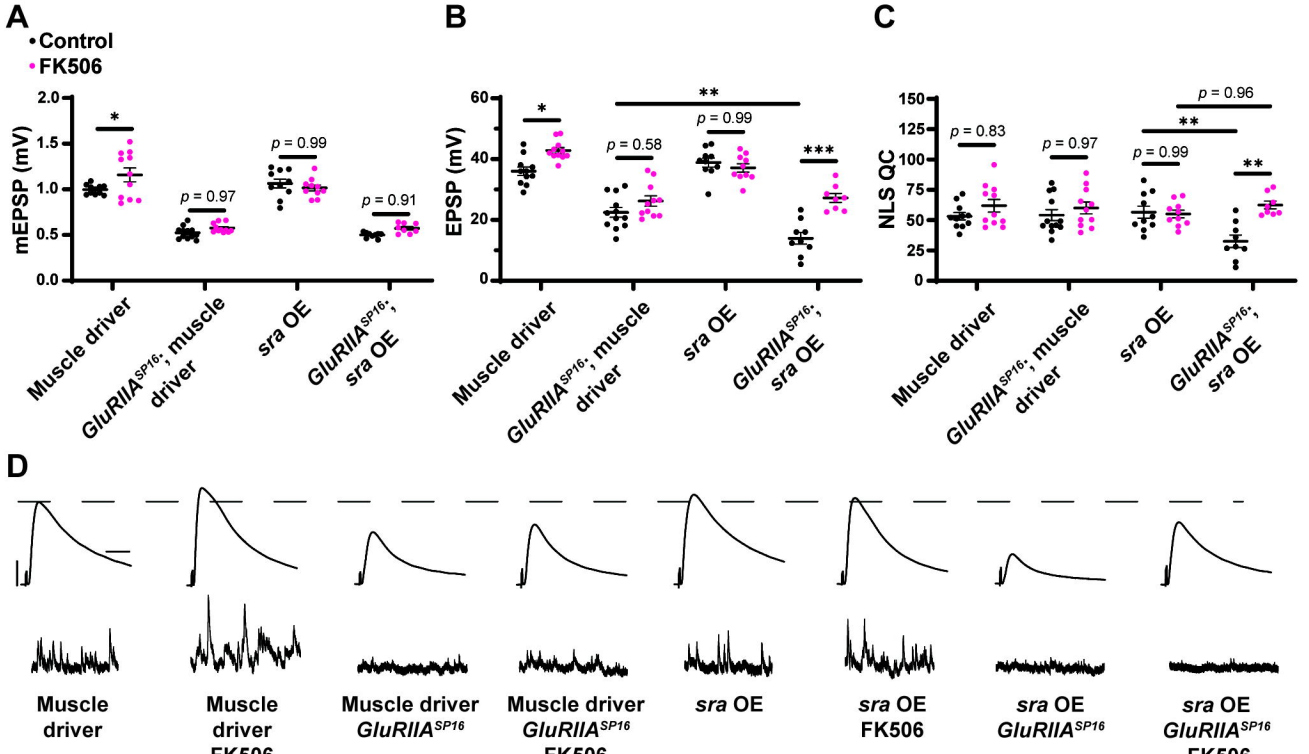
A
Control
FK506
mEPSP (mV)
2.0
1.5
1.0
0.5
0.0
*
p = 0.97
p = 0.99
p = 0.91
Muscle driver
GluRIIA^SP16/+; muscle driver
sra OE
GluRIIA^SP16/+; sra OE
B
EPSP (mV)
60
40
20
0
*
**
p = 0.58
p = 0.99
***
Muscle driver
GluRIIA^SP16/+; muscle driver
sra OE
GluRIIA^SP16/+; sra OE
C
NLS QC
150
125
100
75
50
25
0
p = 0.83
p = 0.97
p = 0.99
p = 0.96
**
**
Muscle driver
GluRIIA^SP16/+; muscle driver
sra OE
GluRIIA^SP16/+; sra OE
D
Muscle driver
Muscle driver FK506
Muscle driver GluRIIA^SP16
Muscle driver GluRIIA^SP16 FK506
sra OE
sra OE FK506
sra OE GluRIIA^SP16
sra OE GluRIIA^SP16 FK506

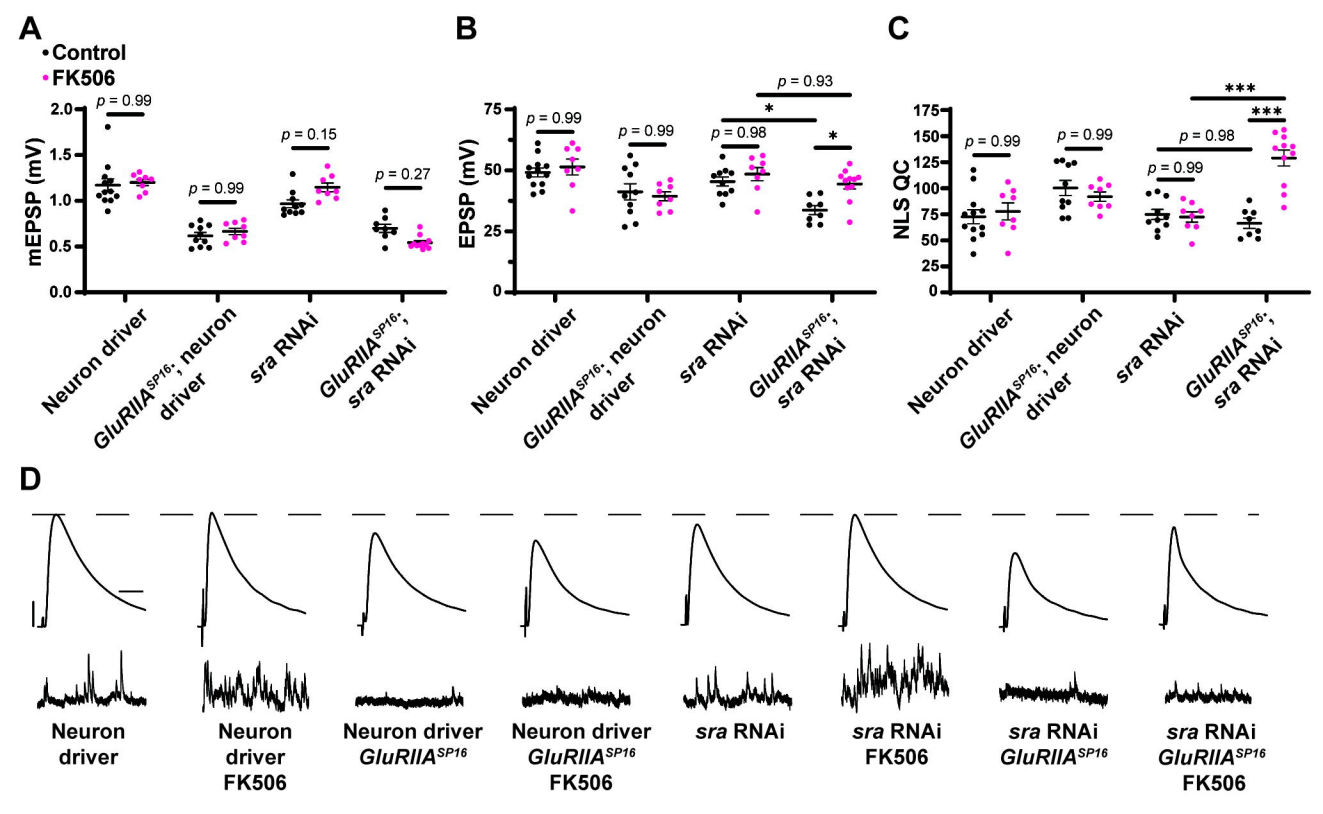
A
Control
FK506
mEPSP (mV)
p = 0.99
p = 0.99
p = 0.15
p = 0.27
Neuron driver
GluRIIA^SP16; neuron driver
sra RNAi
GluRIIA^SP16; sra RNAi
B
EPSP (mV)
p = 0.99
p = 0.99
p = 0.98
p = 0.93
*
*
C
NLS QC
p = 0.99
p = 0.99
p = 0.99
p = 0.98
***
***
D
Neuron driver
Neuron driver FK506
Neuron driver GluRIIA^SP16
Neuron driver GluRIIA^SP16 FK506
sra RNAi
sra RNAi FK506
sra RNAi GluRIIA^SP16
sra RNAi GluRIIA^SP16 FK506

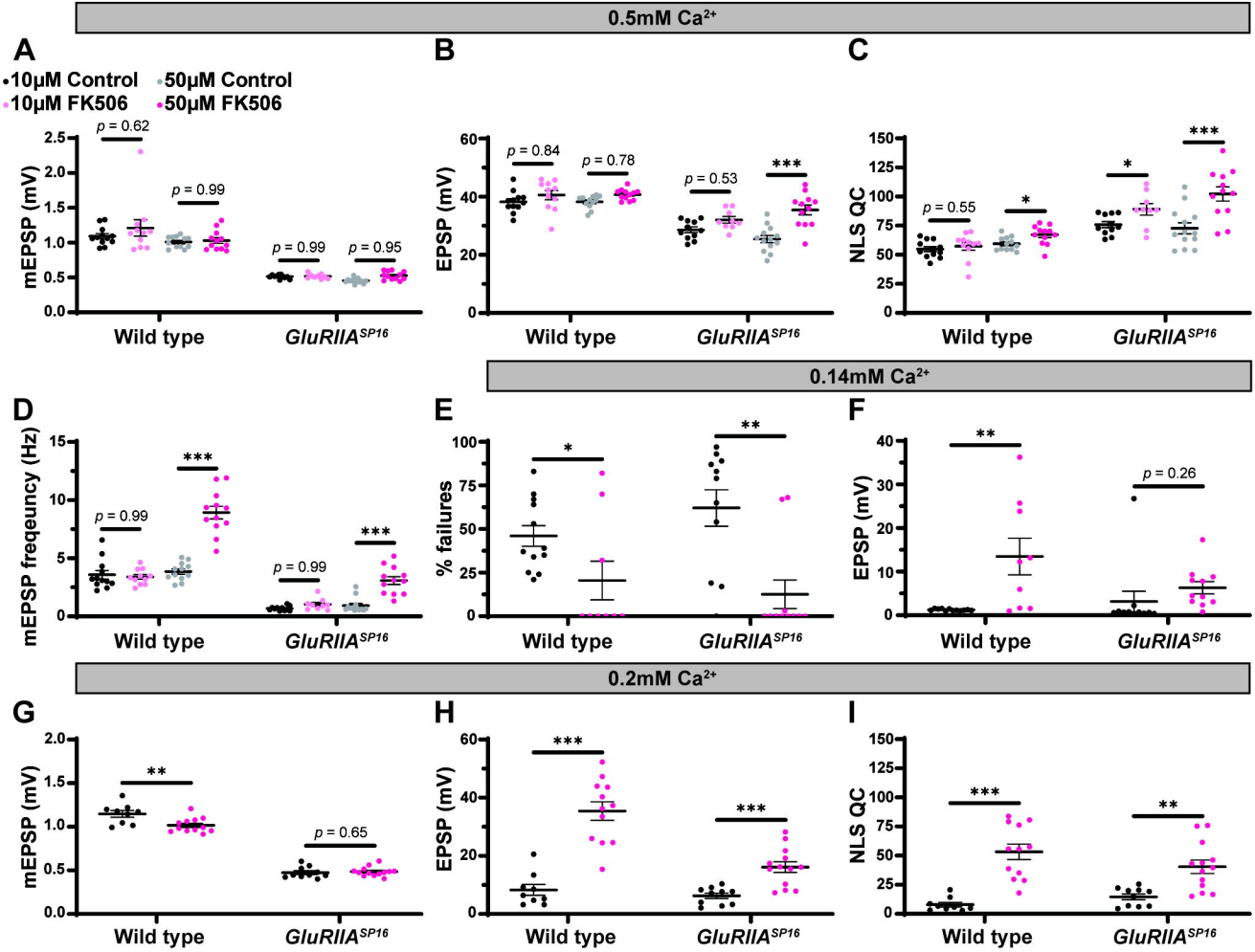
0.5mM Ca2+
A
B
C
10μM Control
50μM Control
10μM FK506
50μM FK506
mEPSP (mV)
EPSP (mV)
NLS QC
p = 0.62
p = 0.99
p = 0.99
p = 0.95
p = 0.84
p = 0.78
p = 0.53
***
p = 0.55
*
*
***
Wild type
GluRIIA SP16
0.14mM Ca2+
D
E
F
mEPSP freqeuncy (Hz)
% failures
EPSP (mV)
p = 0.99
***
p = 0.99
***
*
**
**
p = 0.26
Wild type
GluRIIA SP16
0.2mM Ca2+
G
H
I
mEPSP (mV)
EPSP (mV)
NLS QC
**
p = 0.65
***
***
***
**
Wild type
GluRIIA SP16

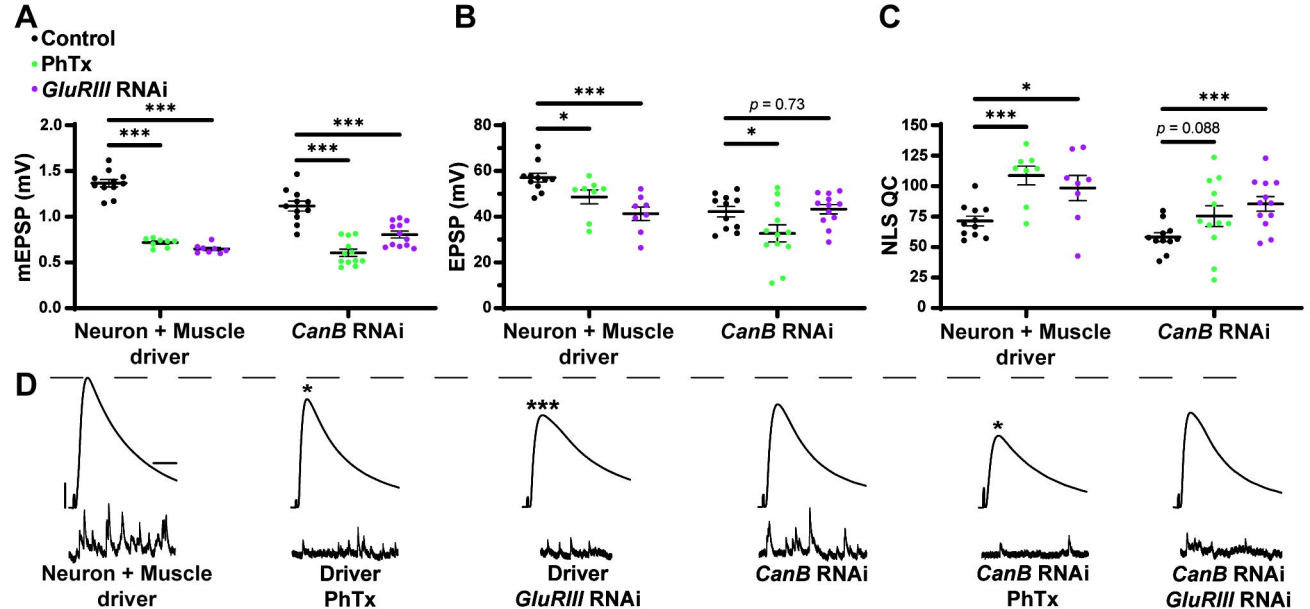
A
Control
PhTx
GluRIII RNAi
mEPSP (mV)
2.0
1.5
1.0
0.5
0.0
***
***
***
***
Neuron + Muscle driver
CanB RNAi
B
EPSP (mV)
80
60
40
20
0
***
*
p = 0.73
*
Neuron + Muscle driver
CanB RNAi
C
NLS QC
150
125
100
75
50
25
0
*
***
***
p = 0.088
Neuron + Muscle driver
CanB RNAi
D
*
***
*
Neuron + Muscle driver
Driver PhTx
Driver GluRIII RNAi
CanB RNAi
CanB RNAi PhTx
CanB RNAi GluRIII RNAi